The Journal of FINANCE
The Journal of THE AMERICAN FINANCE ASSOCIATION

THE JOURNAL OF FINANCE • VOL. , NO. 0 • XXXX 2023

How Integrated are Credit and Equity Markets? Evidence from Index Options

PIERRE COLLIN-DUFRESNE, BENJAMIN JUNGE, and ANDERS B. TROLLE*

ABSTRACT

We study the extent to which credit index (CDX) options are priced consistent with S&P 500 (SPX) equity index options. We derive analytical expressions for CDX and SPX options within a structural credit-risk model with stochastic volatility and jumps using new results for pricing compound options via multivariate affine transform analysis. The model captures many aspects of the joint dynamics of CDX and SPX options. However, it cannot reconcile the relative levels of option prices, suggesting that credit and equity markets are not fully integrated. A strategy of selling CDX volatility yields significantly higher excess returns than selling SPX volatility.

CLASSIC FINANCIAL THEORY VIEWS CORPORATE debt and equity as contingent claims on the firm's underlying asset value (Merton (1974)). Accordingly, credit spreads and equity returns should be tightly connected because they depend on the same set of risk factors in the asset value process. Consistent with

*Pierre Collin-Dufresne is at EPFL and Swiss Finance Institute. Benjamin Junge is at Capital Fund Management. Anders B. Trolle is at Copenhagen Business School. We thank Stefan Nagel (the Editor), the Associate Editor, two anonymous referees, Jack Bao, Jan Ericsson, David Lando, Hugues Langlois, Allan Mortensen, Yoshio Nozawa, Nicki Rasmussen, Martin Scheicher, and seminar participants at the AFA 2022 annual meeting, the CEPR Advanced Forum for Financial Economics, the EFA 2020 annual meeting, the 10th ITAM Finance conference, the second LFE Workshop in Finance at ICEF, the 2021 SFI Research Days, the Virtual Derivatives Workshop, the UCLA Virtual Finance Workshop, Boston University, Erasmus University, Florida International University, HEC Paris, Sharif University of Technology, Tilburg University, Tinbergen Institute, University College Dublin, and University of Zurich for comments and suggestions. Collin-Dufresne gratefully acknowledges support from the Swiss Finance Institute. Trolle gratefully acknowledges support from the Center for Big Data in Finance (Grant no. DNRF167) and the Danish Finance Institute. The authors do not have any conflicts of interest as identified in *The Journal of Finance* disclosure policy.

Correspondence: Anders B. Trolle, Copenhagen Business School, Department of Finance, Solbjerg Plads 3, A4.02, DK-2000 Frederiksberg, Denmark; e-mail: abtr.fi@cbs.dk.

DOI: 10.1111/jofi.13300

much of the literature on structural models, this is how we define "integration" in this paper.[1]

Early tests of first-generation structural models find that these models tend to underpredict the level of credit spreads, especially for investment-grade bonds (Jones, Mason, and Rosenfeld (1984), Huang and Huang (2012)). More complex second-generation structural models, which allow for time-varying risk premia and/or richer asset value dynamics, are more successful at explaining the level of credit spreads (Cremers, Driessen, and Maenhout (2008), Chen, Collin-Dufresne, and Goldstein (2009), Du, Elkamhi, and Ericsson (2019)). In particular, Cremers, Driessen, and Maenhout (2008) demonstrate a close connection between credit spreads and prices of equity index options. More recently, Culp, Nozawa, and Veronesi (2018) propose the use of equity options and contingent-claim pricing to construct "pseudo firms" whose derived credit spreads they find to be consistent with actual credit spreads, suggesting "a good deal of integration between corporate bond and options markets."[2]

In this paper, we extend the question of integration between credit and equity markets to higher-order moments by investigating whether, in addition to credit spreads, structural models can also match the relative prices of credit and equity index options. Specifically, we use a novel data set of options on a broad credit index to infer implied credit volatilities across a range of moneyness and maturities. We characterize the dynamics of the resulting credit-implied volatility surface and its relation to the volatility surface obtained from equity index options, and we explore whether the two surfaces and their time variation are consistent when examined through the lens of a rich structural model.

Credit indexes constitute the most liquid component of the corporate credit derivatives market.[3] We focus on the credit index for North American investment-grade firms—the CDX.NA.IG, henceforth CDX. The years after the financial crisis saw the development of an active market for credit index options, and our first contribution is to characterize the trading activity in CDX options since trade reporting became mandatory at the end of 2012. Trades are generally large, with about two-thirds of the trades having a notional amount of the underlying CDX that is at or above the level for which the reported notional is capped (typically either USD 100 million or USD 110 million).[4] We estimate that the average daily trading volume during our sample period was USD 4.35 billion, but trading volume exhibits an upward trend and peaks at the height of the COVID-19 crisis in March 2020, where we estimate that it

[1] Admittedly this is a restrictive definition. A broader definition of integration might only require that all prices are compatible with a common pricing kernel; see, e.g., Chen and Knez (1995) and Sandulescu (2020).

[2] See Culp, Nozawa, and Veronesi (2018, p. 458).

[3] See Collin-Dufresne, Junge, and Trolle (2020) for a detailed description of this market.

[4] Trading between clients and dealers takes place almost exclusively over the counter, while interdealer trading often takes place on dedicated trading platforms. For the subset of trades that are executed on the main interdealer trading platform, we have additional data from which we can infer that the capped trades on that platform have an average notional of USD 353 million.

reached an average of USD 11.08 billion per day. In the vast majority of option trades, the underlying is the five-year on-the-run (i.e., most recently issued) CDX contract, and these options are the focus of the paper. We further show that trading activity is concentrated in relatively short-term (up to three to four months) options, and that there is relatively more trading in high-strike options, which pay off when credit spreads are high.

We next use composite dealer quotes to characterize the pricing of CDX options and the relation to S&P 500 (SPX) options.[5] CDX implied volatility smiles are consistently positively skewed, which is economically consistent with the well-known negative skew of SPX implied volatility smiles because CDX options are quoted in terms of implied credit-spread volatilities, and credit spreads and equity values are negatively related. Therefore, the positive (negative) skews of credit (equity) implied volatility smiles reflect a higher premium for options that pay off in adverse economic states, when credit spreads are high and equity values are low.

We also investigate the joint dynamics of the underlying index, volatility, and skewness, both within each market and across markets. We find that much like CDX and SPX returns are highly (negatively) correlated, the smile dynamics are also correlated. Specifically, at-the-money (ATM) CDX and SPX implied volatilities are highly positively correlated, while the skewness of CDX and SPX volatility smiles are negatively correlated.

Since the model-independent analysis shows a strong connection between CDX and SPX options, we next examine whether they can be linked through a rich structural credit-risk model. We consider a general specification for the asset value dynamics of a representative index constituent in which both idiosyncratic and systematic risk have a diffusive component and a jump component. In addition, the common factor exhibits stochastic volatility and a variance-dependent jump intensity. We allow for both short-term and long-term debt in order to generate a term structure of credit spreads. Indexes and index options are given as compound options, and we develop new results on multivariate transform analysis for affine processes to price these options analytically, thereby facilitating our empirical analysis.[6]

We estimate the model using data at a weekly frequency on the CDX term structure, the SPX level, and the SPX option surface (as well as short-term and long-term index leverage ratios and the index dividend yield), and then price the CDX option surface out-of-sample. Consistent with the data, the fitted CDX implied volatility surfaces are consistently positively skewed.

[5] We follow standard market practice and express CDX option prices in terms of log-normal implied credit-spread volatilities using a reduced-form model.

[6] Our model builds on the classic structural approach to pricing corporate debt (Merton (1974), Geske (1977)). Carr and Wu (2010) propose a "hybrid" pricing framework in which credit default swaps (CDSs) are priced using a reduced-form approach given an exogenous default intensity and equity options are priced using standard transform analysis applied to the underlying default-adjusted stock price process. This is unlike in traditional structural models, where the stock price, bond price, and default time are determined endogenously by the dynamics of the underlying asset value process.

Moreover, the magnitude and variation in skewness generated by the model is similar to that observed in the data. The model also largely replicates the joint index-volatility-skewness dynamics observed in the data, both within the CDX market and across the two markets.

However, the model cannot match the level of the CDX implied volatility surfaces. Indeed, the CDX implied volatilities generated by the model are, on average, 28% lower than those observed in the market. Viewed through the lens of the model, this price difference suggests that market prices of CDX options are too expensive relative to SPX options, indicating that credit and equity markets are not fully integrated.[7]

We explore the robustness of our findings along several dimensions. First, our model assumes an infinite number of homogeneous constituents in the two indexes—the "large homogeneous pool" (LHP) approximation of Vasicek (1987)—in order to obtain analytic pricing formulas. We extend the model and perform numerical analyses to investigate the effects of heterogeneity and a finite number of index constituents, and find that these extensions are unlikely to explain our empirical results.

Second, while our analysis does not require the two indexes to be identical in terms of constituents, it requires a high degree of similarity in terms of index risk characteristics. We compare the two indexes in terms of the distributions of rating, leverage, and total and systematic asset return volatility across constituents—four characteristics that are central to our structural model. We find the distributions to be very similar in terms of mean and median values, even though the SPX distributions display more dispersion. In particular, because index option prices are increasing in systematic asset volatility, one potential resolution of the observed price differential for CDX options could be higher average systematic asset volatility among CDX constituents, but we find it to be marginally lower.

Third, the relative valuation analysis requires that the two sets of option contracts span similar economic states. By converting option strikes to a common scale, namely, expressing strikes in terms of asset value, we show that this is indeed the case.

Finally, we corroborate our results on the relative valuation of CDX and SPX options by comparing the profitability of selling volatility in the two markets. We show that a strategy of selling CDX volatility yields significantly higher average excess returns and Sharpe ratios than selling SPX volatility.[8] A short-long strategy of selling CDX volatility versus buying SPX volatility also generates a high Sharpe ratio, although lower than what is attained by selling CDX volatility outright. However, its higher-order moments are more

[7] We also consider the reverse estimation approach, where we fit to the CDX option surface and price the SPX option surface out-of-sample. Consistent with our main analysis, in this case the model fails to match the level of the SPX implied volatility surface.

[8] For instance, a strategy of selling an equally weighted portfolio of option straddles (appropriately sized) yields a Sharpe ratio of 1.744 in the CDX market compared to a Sharpe ratio of 0.659 in the SPX market.

attractive, with the return distribution being roughly symmetric (instead of highly negatively skewed) and much less leptokurtic.

In the conclusion, we discuss several possibilities for follow-up research. Clearly, in interpreting our results, we face the joint hypothesis problem (e.g., Fama (1970)) that we can never definitively tell whether the results reflect lack of integration between the two markets or model misspecification. Although our model incorporates salient features of asset value dynamics, it would be relevant to explore whether our findings hold true in various model extensions. Adding credit-specific factors to the model seems particularly promising, and we suggest one such extension—systematic variation in bankruptcy costs—and show how it can be incorporated in our model.

Another possibility is that there are institutional features that can lead to market segmentation and distort the relative prices of index options. For instance, even if CDX and SPX options are close substitutes, they are not treated as such by regulators in the context of credit-risk hedging by financial institutions. We provide suggestive evidence for significant regulatory-driven demand from banks for CDX options. However, quantifying such demand and linking it to variation in the relative valuation of index options is left for future research.

The paper is related to several strands of literature. The model is related to Bai, Goldstein, and Yang (2019), who focus on pricing equity index options in a structural model using the LHP approximation. Relative to their paper, we also treat credit index options, allow option expiries to differ from debt maturity (thereby treating options as true compound options on the firm asset value), and derive full analytical solutions to option prices in a more general stochastic-volatility jump-diffusion setting using new results on multivariate transform analysis for affine processes.[9] Our results on multivariate transform analysis generalize the univariate analysis of Duffie, Pan, and Singleton (2000) and have many applications beyond our specific use in this paper for valuing compound options.[10]

In contrast to the aforementioned papers on the level of credit spreads, a number of papers provide evidence that points toward imperfectly integrated equity and corporate credit markets. Collin-Dufresne, Goldstein, and Martin (2001) find that a large fraction of changes in credit spreads cannot be explained by variables suggested by the Merton (1974) model. The unexplained residuals seem to be driven by few common factors that subsequent papers have linked to illiquidity factors (Friewald and Nagler (2019)) or intermediary balance-sheet factors (He, Khorrami, and Song (2022)). A number of recent papers (Chordia et al. (2017), Choi and Kim (2018), and Bai, Bali, and Wen (2019)) document differences in the set of factors and characteristics that explain the cross sections of corporate bond and stock returns. Schaefer and

[9] Allowing option expiries to differ from debt maturity is important in our setting in which option expiries are typically less than four months while the underlying credit index has a maturity of approximately five years. Bai, Goldstein, and Yang (2019) derive option prices up to an expectation that is computed via numerical integration.

[10] For instance, our results can be used to value complex "cliquet outperformance options" (options that depend on the maximum realization of one or several prices at various fixed dates prior to the option maturity) in general affine models.

Strebulaev (2008) find that the Merton (1974) model produces reasonable sensitivities of bond returns to stock returns, although a sizable excess bond return volatility remains, which Bao and Pan (2013) link to time-varying bond illiquidity. Kapadia and Pu (2012) find short-lived divergences between CDS and stock prices, especially for firms with high arbitrage costs. A common feature of all these papers is that they study bond returns or credit spread changes of individual firms, for which illiquidity effects are likely to be important. In contrast, we focus on a highly liquid credit index and its options.

Finally, the paper is related to a recent literature on the relative pricing of CDX tranche swaps and SPX options (Coval, Jurek, and Stafford (2009), Collin-Dufresne, Goldstein, and Yang (2012), and Seo and Wachter (2018)). In principle, this literature also provides insights into the integration of equity and credit derivatives markets. However, in practice the relative pricing of these instruments is complicated by several factors: (i) CDX tranche swaps are long-dated contracts while the most liquid SPX options have short expiries,[11] (ii) the range of (negative) economic states spanned by CDX tranche swaps is much wider than that spanned by SPX options (Collin-Dufresne, Goldstein, and Yang (2012)), and (iii) trading in CDX tranche swaps has languished after the financial crisis. In contrast, CDX and SPX options are much more closely aligned in terms of which option maturities are liquid and the range of economic states that are spanned. Moreover, CDX options have flourished since the financial crisis.[12]

The paper is structured as follows. Section I describes the CDX options market and the transaction and quote data. Section II characterizes the relation between CDX and SPX options. Section III presents the structural model, Section IV shows how to use multivariate transform analysis for affine processes to price indexes and index options, Section V describes model estimation and results, and Section VI discusses robustness checks. Section VII concludes. Proofs are given in the Appendix, and an Internet Appendix contains supplementary results.[13]

I. CDX and CDX Options

A. CDX

A credit index is a CDS that provides default protection on a set of companies belonging to an index, with the notional of the swap divided evenly among the index constituents. We focus on the investment-grade CDX that provides default protection on 125 investment-grade companies. CDX contracts are issued with initial maturities between one and ten years. A new set of CDX

[11] This literature, therefore, uses less liquid long-term SPX options that are traded over the counter.

[12] Based on all (capped) trade reports since 2013 and aggregating across all North American credit indexes, we find that trading volume in tranche swaps is only 9% of the trading volume in options.

[13] The Internet Appendix may be found in the online version of this article.

contracts referencing a "refreshed" index is issued every March and September.[14] The most recently launched contracts are called on-the-run; all previously launched contracts are referred to as off-the-run. Most trading activity is in the five-year on-the-run contract. Virtually all such trades are centrally cleared and executed on dedicated trading platforms (so-called swap execution facilities or SEFs) at very low transaction costs. See Collin-Dufresne, Junge, and Trolle (2020) for details about the market structure and transaction costs of CDX.

Coupon payments in a CDX contract are standardized and occur at a fixed rate of 100 basis points (bps) per year.[15] The present value of the premium leg, therefore, typically does not correspond to the present value of the protection leg, which reflects the market's perceived credit risk of the underlying index constituents. As a consequence, when entering the contract, the buyer of protection pays an upfront amount equal to the difference between the present values of the two legs. However, traders usually quote a CDX contract in terms of a "par spread," which is the fixed coupon rate that would be required for the upfront amount to be zero. There is a one-to-one correspondence between upfront amount and par spread, and market participants conventionally use the ISDA CDS Standard Model for the conversion, as we explain in more detail in Section I of the Internet Appendix.[16]

When an index constituent defaults, the loss is settled in the same way as a single-name CDS, and the outstanding notional of the swap is reduced. From then on, the swap references a new version of the index without the defaulted name.

B. CDX Options

A CDX option is an option to enter into a CDX contract at a given strike price. A payer option gives the right to buy credit protection (paying the strike and the subsequent coupons) while a receiver option gives the right to sell credit protection (receiving the strike and the subsequent coupons). Options are European style and are quoted for a wide set of strikes and monthly expirations. Options expire on the third Wednesday of each month. Contractually, the option payoff is given in upfront terms. For quotation purposes, however, it is standard practice to write the payoff in spread terms and express the option price as a log-normal spread implied volatility. Details—including how

[14] These *roll dates* are March 20 and September 20 (in the second half of 2014, the roll date was postponed to October 6 due to delays in signing up market participants to the 2014 International Swaps and Derivatives Association (ISDA) Credit Derivatives Definitions). The index constituents are selected from the investment-grade companies that have the most liquid single-name CDSs traded on them. Each index is identified by its series number.

[15] Throughout the paper, we assume that coupons are paid continuously at a rate of $C =$ 100 bps, which greatly simplifies notation. In reality, coupons are paid quarterly on standardized coupon dates.

[16] Note that the upfront amount can be negative, in which case the par spread will be less than the fixed coupon rate.

Table I
Descriptive Statistics for CDX and CDX Option Trades

The table shows descriptive statistics for CDX and CDX option trades. Tenor is the initial time to expiration of the CDX contract (the underlying CDX contract in the case of CDX options). The on-the-run series is the most recently launched CDX contract. Typically, reported trade sizes are capped when the notional amount traded exceeds USD 100 million or USD 110 million. The sample period is December 31, 2012 to April 30, 2020. The sample comprises 371,693 CDX trades and 32,669 CDX option trades.

	CDX	CDX Options
Trades per day	202	18
Median trade size (in million USD)	50	100
Capped trade size (% of trades)	22.3	66.5
Average daily volume (in million USD)	11,133	1,442
Five-year tenor (% of trades)	96.1	98.1
On-the-run series (% of trades)	88.9	94.0
On-SEF execution (% of trades)	83.9	3.8
Cleared (% of trades)	90.4	17.6
Payer (% of trades)	—	63.1

defaults during the life of the option are handled—are provided in Section I of the Internet Appendix. Note that a payer (receiver) option is a call (put) option on the upfront/spread.

C. Trading in CDX Options

To understand the trading activity in CDX options, we analyze all reported transactions from December 31, 2012 (when reporting to swap data repositories became mandatory) to the end of our sample period on April 30, 2020. Table I displays descriptive statistics of the transaction data. For completeness, the table also reports statistics on CDX transactions. In contrast to CDX, trading in CDX options takes place predominantly over the counter, and the SEF trades that we do observe are almost exclusively interdealer trades. Central clearing is also less prevalent in CDX options than in CDX.[17]

CDX option trades are relatively infrequent (18 trades per day, on average) but large in size (measured in terms of the notional amount of the underlying CDX). The median of the reported trade sizes is USD 100 million. However, about two-thirds of the trades are reported with a capped notional, which implies that trade sizes are typically much larger.[18] For the subset of trades that take place on the main interdealer trading platform (GFI SEF), we have

[17] For CDX, five-year on-the-run (and immediate off-the-run) trades are, with a few exceptions, required to be executed on SEFs and to be centrally cleared. For CDX options, there are no such requirements.

[18] The level of the cap is determined by the Commodity Futures Trading Commission and varies over time and with option strike. In most trade reports, the notional is capped at either USD 100 million or USD 110 million.

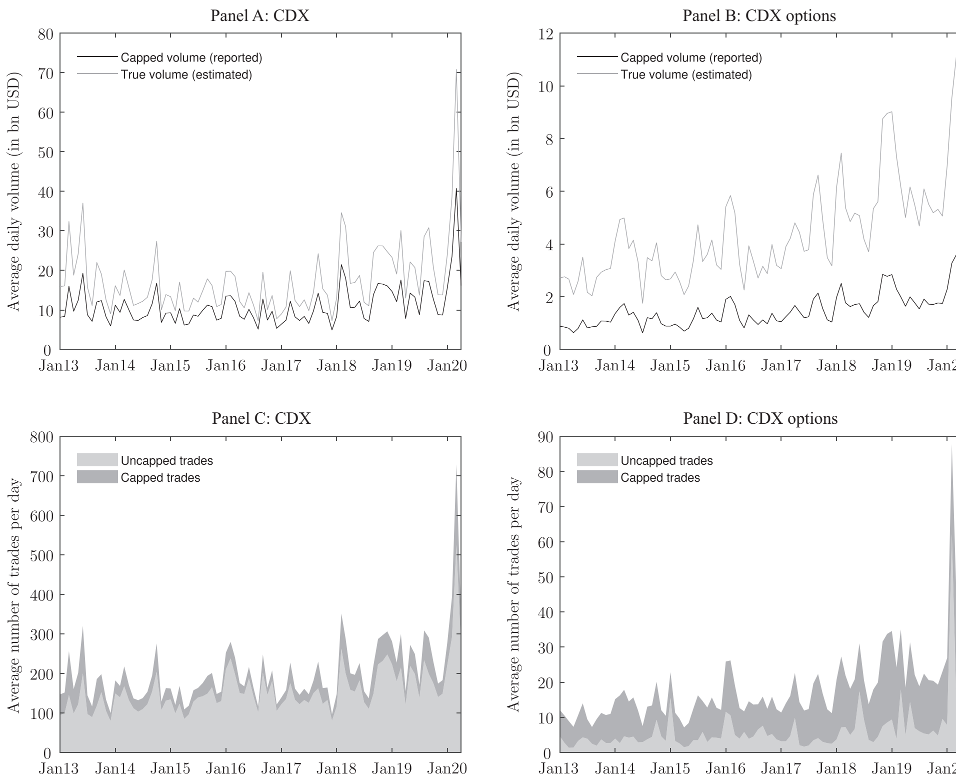

Figure 1. Trading activity for CDX and CDX options. Panels A and B show the average daily trading volume for CDX and CDX options. Panels C and D show the average number of trades per day for CDX and CDX options. Daily market activity reports from the GFI SEF are used to compute the average amount by which the actual notionals of capped trades on the GFI SEF exceed the reported notionals. This is done separately for CDX and CDX options (see footnote 19 for details). The estimated true volume in Panels A and B is obtained by adding the average amount to the reported notionals for all capped trades. The frequency of observations is monthly. The sample period is December 31, 2012 to April 30, 2020 (88 observations).

additional data from which we can infer that the capped trades in that subset have an average size of USD 353 million.[19] The average daily trading volume based on the capped trade reports is USD 1.44 billion. Assuming that all capped trades exceed their reported notionals by the same amount as on the GFI SEF, we obtain an estimate of the true average daily trading volume

[19] Daily market activity reports from the GFI SEF show that the aggregate uncapped notional amount traded is USD 108,410 million for CDX options during the period from October 2, 2013 to April 30, 2020. Identifying GFI SEF trades in the transaction data shows that the aggregate capped notional amount is USD 34,829 million, and that there are 300 capped trades with an average reported notional of USD 108 million. This implies that these capped trades have an average size of USD 353.27 (=108 + (108,410 − 34,829)/300) million.

Table II

Distribution of Trading Volume across the CDX Volatility Surface

The table shows the percentage of CDX option volume across the volatility surface. Moneyness is defined as $m = \log(K/F(\tau))/(\sigma\sqrt{\tau})$, where K is the strike, $F(\tau)$ is the front-end-protected τ-forward spread, σ is at-the-money implied volatility, $\tau = d/365$ is time to expiration, and d is days to expiration. The underlying of all options is the five-year on-the-run index. The sample period is December 31, 2012 to April 30, 2020. The sample comprises 28,409 CDX option trades.

	Days to Expiration						
Moneyness	<15	15–44	45–74	75–104	105–134	≥135	Total
$m < -1.5$	0.20	0.24	0.06	0.01	0.00	0.00	0.52
$-1.5 \leq m < -0.5$	0.94	3.99	2.94	1.62	0.54	0.39	10.42
$\lvert m\rvert \leq 0.5$	2.12	15.28	9.61	6.48	2.27	1.28	37.03
$0.5 < m \leq 1.5$	1.53	9.01	10.34	8.75	4.17	2.30	36.10
$m > 1.5$	1.42	5.96	4.45	2.65	0.97	0.47	15.92
Total	6.21	34.47	27.40	19.51	7.95	4.45	

of USD 4.35 billion.[20] Note that this is a downward-biased estimate because the trade reporting requirement only pertains to trades for which at least one counterparty is a U.S. institution.

Figure 1 displays the evolution in trading activity on a monthly basis. Panels A and B show the average daily trading volume for CDX and CDX options, respectively, while Panels C and D show the average number of trades per day. Underscoring the growing popularity of CDX options, trading volume exhibits an upward trend during the sample period. The average daily trading volume based on the capped trade reports (estimated true volume) increased from USD 0.88 billion (USD 2.72 billion) in January 2013 to USD 2.08 billion (USD 6.23 billion) in April 2020. Trading volume peaks at the height of the COVID-19 crisis in March 2020 at USD 3.59 billion (USD 11.08 billion) per day. The highest trade count for CDX options is in February 2020 at 88 trades per day, on average.

Table I shows that in the vast majority of option trades, the underlying CDX is the five-year on-the-run contract. We therefore focus on those options in the remainder of the paper.

Table II shows the distribution of trading volume across moneyness and option maturity. We define moneyness as

$$m = \frac{\log\left(\frac{K}{F(\tau)}\right)}{\sigma^{ATM}\sqrt{\tau}}, \tag{1}$$

[20] Compared with CDX option trades, CDX trades are more frequent (202 trades per day, on average) but smaller in size, with a median trade size of USD 50 million and less than a quarter of the trade sizes being above the cap. The average daily trading volume based on the capped trade reports is USD 11.13 billion but we estimate that the true volume is USD 17.80 billion using the same method as for CDX options.

where K is the strike, $F(\tau)$ is the forward spread, σ^{ATM} is the ATM log-normal spread implied volatility, and τ is the maturity. Intuitively, m measures the number of standard deviations that an option is in or out of the money given log-normally distributed spreads. The table shows that there is more trading in high-strike than low-strike options. It also shows that trading is concentrated in relatively short-term options with maturities out to three to four months.

D. CDX Option Quotes

To have synchronized data across the option surface, we use quotes rather than trades. Specifically, we use end-of-day composite dealer quotes from Markit.[21] The sample period is from February 24, 2012 to April 30, 2020.

Details on the quote data are given in Sections II and III of the Internet Appendix. There we find that when option maturities become very short (typically less than one week), dealers stop quoting prices. Beyond that, there are almost always quotes for at least three monthly expirations. At longer maturities, quotes are more sporadic. In light of these findings as well as the evidence on option transactions in Table II, on each observation date we select the first three monthly expirations among the options that have more than two weeks to expiration. These options are denoted M1, M2, and M3. The average option maturities are 29.9, 60.2, and 90.6 calendar days, respectively.

For each maturity, we consider 13 moneyness "buckets": $-3.25 < m \leq -2.75$, $-2.75 < m \leq -2.25, \ldots, 2.75 < m \leq 3.25$, where m is defined in (1). Within each bucket, we search for the option that is closest to the midpoint of the interval. We only search among out-of-the-money (OTM) options due to their higher liquidity. In the ATM category, we give priority to payer options.

The result of this data-sorting is a uniform maturity-moneyness grid that preserves the information in the data without overweighing those dates on which more maturities and/or strikes are quoted. In the Internet Appendix, we show that quotations are tilted toward higher-strike options. This probably reflects both the higher interest in trading those options (see Table II) and the fact that the risk-neutral spread distribution is heavily skewed toward higher spreads (see below) so that deep OTM payer options (by our moneyness measure) have meaningful prices even when deep OTM receiver options have little value.

E. SPX Option Quotes

SPX options trade on the Chicago Board Options Exchange (CBOE), from which we obtain end-of-day quotes. Regular SPX options expire on the third Friday of each month (there are also weekly and end-of-month expirations that we do not consider). On each observation date, we search for the three SPX option maturities that are closest to the three CDX option maturities. These SPX options expire either two days after or five days before and hence there

[21] Markit is arguably the leading data provider for credit derivatives. According to the "Markit Credit Options" user guide, the "credit index option composite is calculated from quotes received from market makers."

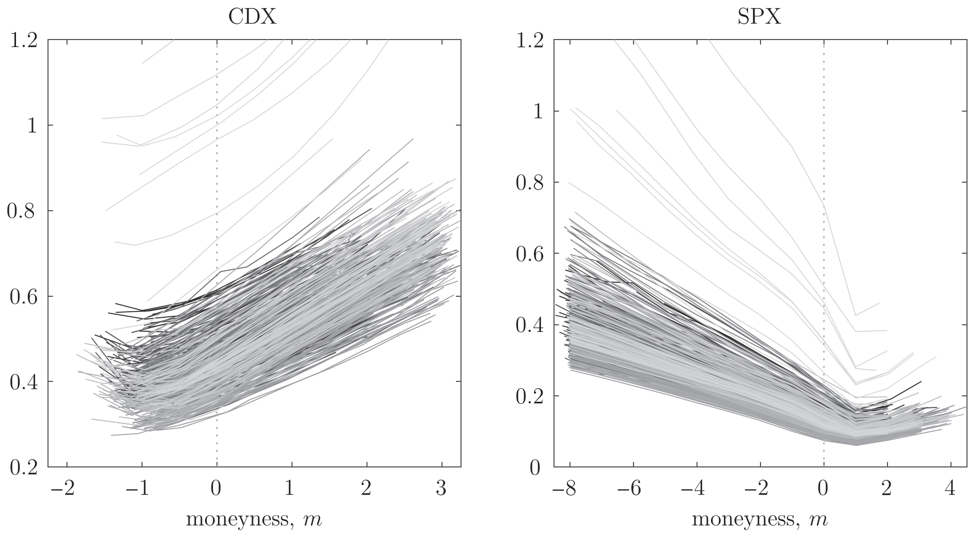

Figure 2. CDX and SPX implied volatility smiles. The figure shows weekly (Wednesday) two-month implied volatility smiles for CDX and SPX. CDX data are displayed in the left panel and SPX data are displayed in the right panel. Moneyness is defined as $m = \log(K/F(\tau))/(\sigma\sqrt{\tau})$, where K is the strike, $F(\tau)$ is the forward (front-end-protected) spread in the case of CDX options and the forward price in the case of SPX options, σ is the at-the-money implied volatility, and τ is the maturity of the option. The sample period is February 29, 2012 to April 29, 2020 (427 observations).

is a close match in maturity between SPX and CDX options. The average SPX option maturities are 30.6, 61.2, and 91.5 calendar days, respectively.

For each maturity, we next find the OTM options that are closest to the midpoints of the following 13 moneyness intervals: $-8.5 < m \leq -7.5$, $-7.5 < m \leq -6.5$,..., $3.5 < m \leq 4.5$, where m is again defined in (1), but with $F(\tau)$ denoting the forward SPX value. Note that the m-range is not directly comparable across CDX and SPX options (one is in spread terms while the other is in price terms). Rather, given the m-range for CDX options, we choose the m-range for SPX options so that the moneyness range is roughly similar when expressed on a common scale, namely, in asset-value terms; see Section VI.C.

II. Stylized Facts

To provide an initial sense of the data, Figure 2 shows weekly CDX and SPX implied volatility smiles for the two-month maturity. Weekly data are sampled each Wednesday.[22] It is immediately apparent that implied volatility smiles for CDX options are positively skewed, in contrast to the negatively skewed SPX implied volatility smiles. This is economically intuitive in that adverse economic states are characterized by low equity prices and high credit spreads.

[22] If Wednesday is not a trading day, we consider the preceding Tuesday instead. The sample comprises 427 weekly observation dates from February 29, 2012 to April 29, 2020.

Therefore, if such states carry a high risk and/or price of risk, prices of OTM SPX put options and OTM CDX call options will be elevated.

To summarize the information in implied volatilities across moneyness, option maturity, and time, we follow the approach in Foresi and Wu (2005). On each date and for each option maturity, we run the cross-sectional regression

$$\sigma^{IV}(m) = \beta_0 + \beta_1 m + \beta_2 m^2 + \epsilon, \tag{2}$$

where m is the measure of moneyness given in (1) and ϵ is an error term. In this regression, β_0 captures the ATM implied volatility, β_1 captures the skewness of the implied volatility smile, and β_2 captures the curvature of the implied volatility smile. The β-coefficients are highly correlated across option maturity. Therefore, for ease of exposition, we average the β-coefficients across option maturity to produce single time series of β_0, β_1, and β_2. Note that β_2 is sensitive to the moneyness range, which varies over time, especially for CDX options (see Figure IA3 in the Internet Appendix). This variation introduces noise in the estimate of curvature. For this reason, we mainly focus on the dynamics of volatility and skewness.

Figure 3 provides an overview of the data with the left (right) panels showing data for the CDX (SPX) market. The top-left panel shows time series of the 1Y and 5Y CDX spreads. Normally, the CDX term structure is strongly upward-sloping. During the COVID-19 crisis, however, the slope flattens as the 1Y spread increases more than the 5Y spread. At the peak of the crisis, the 5Y spread reaches 151 bps.

The middle-left panel (blue line) shows the time series of CDX volatility. Clearly, CDX volatility exhibits significant variation. In particular, it spikes during the COVID-19 crisis in March 2020, when it reaches a maximum of 1.35 relative to the sample average of 0.47. Moreover, variation in CDX and SPX volatility (middle-right panel) appears to be highly positively correlated.

The lower-left panel (blue line) shows the time series of CDX skewness. This confirms the observation in Figure 2 that the CDX implied volatility smiles are always positively skewed. CDX skewness varies over time and reaches a maximum of 0.149 during the COVID-19 crisis relative to a sample average of 0.073. It appears that variation in CDX and SPX skewness (lower-right panel) is moderately negatively correlated so that, when the SPX volatility smile becomes more skewed toward OTM put options, the CDX volatility smile tends to become more skewed toward OTM call options.[23]

We next investigate more formally the joint dynamics of the underlying index, volatility, and skewness, both within each market and across markets. To this end, the left part of Table III reports correlations (in weekly changes) between the log CDX spread, CDX volatility, CDX skewness, log SPX index, SPX volatility, and SPX skewness. To ensure that our findings are not driven by the

[23] One exception is during the COVID-19 crisis. Initially, both CDX and SPX skewness become more pronounced, but CDX skewness already reverses on March 9 while SPX skewness reverses on March 18. Figure IA11 in the Internet Appendix shows the smile dynamics during the COVID-19 crisis.

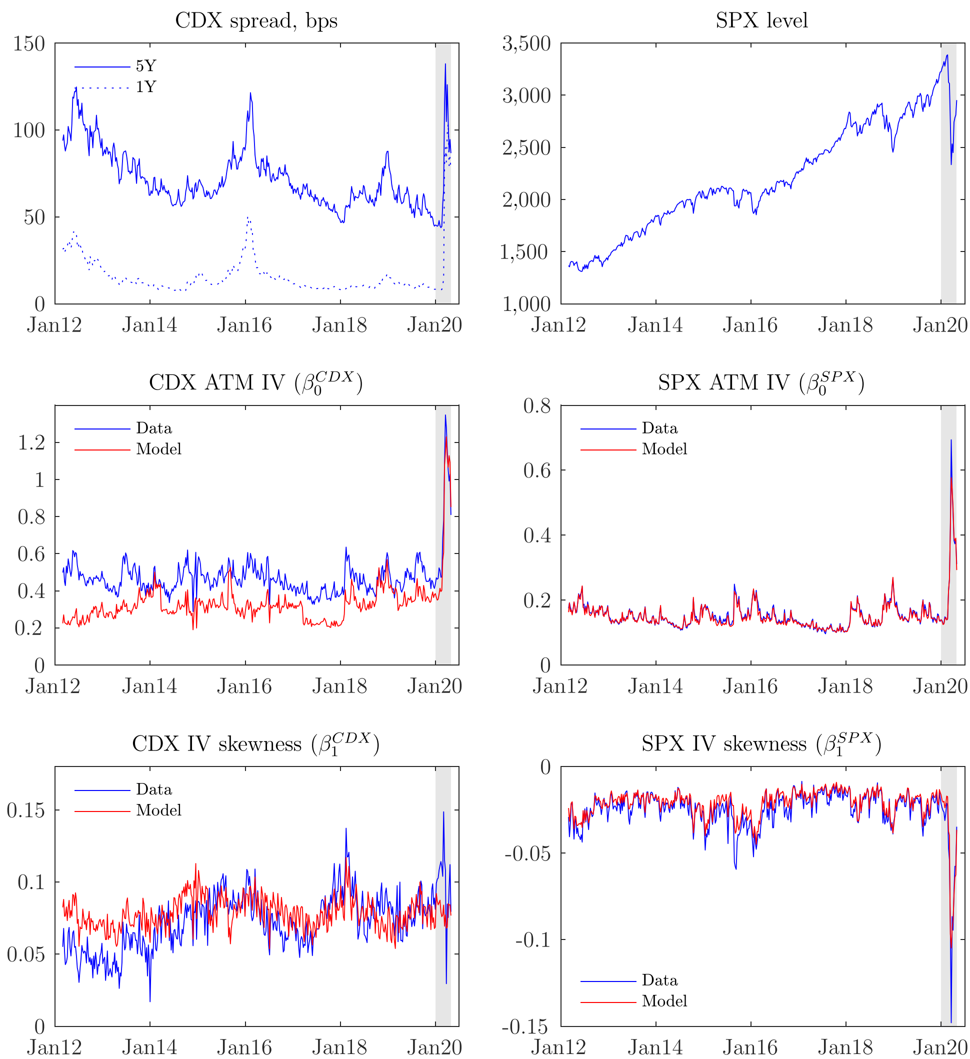

Figure 3. Key metrics in CDX and SPX options markets. The top left (right) panel shows time series of the CDX spread (SPX level). The middle left (right) panel shows time series of the at-the-money CDX (SPX) implied volatility proxied by β_0. The bottom left (right) panel shows time series of the skewness of the CDX (SPX) implied volatility smile proxied by β_1. Blue lines show the data. Red lines show the fitted data for the model calibrated to SPX options. The sample period is February 29, 2012 to April 29, 2020 (427 weekly observations). The shaded area marks the COVID-19 period starting on January 1, 2020.

Table III

Correlations within and across Markets

The table reports correlations between weekly changes in the log CDX spread (ΔI^{CDX}), CDX volatility ($\Delta\beta_0^{CDX}$), CDX skewness ($\Delta\beta_1^{CDX}$), log SPX index (ΔI^{SPX}, i.e., the log SPX return), SPX volatility ($\Delta\beta_0^{SPX}$), and SPX skewness ($\Delta\beta_1^{SPX}$). The correlation matrices to the left ("Data") are computed from the data, and those to the right ("Model") are computed from the fitted data using the model calibrated to SPX options. The full sample period is February 29, 2012 to April 29, 2020 (427 weekly observations). The ex-COVID-19 sample period is February 29, 2012 to December 31, 2019 (410 weekly observations).

Panel A: Full Sample

	Data					Model				
	ΔI^{CDX}	$\Delta\beta_0^{CDX}$	$\Delta\beta_1^{CDX}$	ΔI^{SPX}	$\Delta\beta_0^{SPX}$	ΔI^{CDX}	$\Delta\beta_0^{CDX}$	$\Delta\beta_1^{CDX}$	ΔI^{SPX}	$\Delta\beta_0^{SPX}$
$\Delta\beta_0^{CDX}$	0.62					0.49				
$\Delta\beta_1^{CDX}$	0.20	0.39				0.11	0.22			
ΔI^{SPX}	−0.80	−0.65	−0.23			−0.80	−0.60	−0.11		
$\Delta\beta_0^{SPX}$	0.67	0.69	0.22	−0.86		0.68	0.83	0.12	−0.85	
$\Delta\beta_1^{SPX}$	−0.65	−0.58	−0.33	0.74	−0.80	−0.68	−0.68	−0.25	0.70	−0.74

Panel B: Ex-COVID-19 Sample

	Data					Model				
	ΔI^{CDX}	$\Delta\beta_0^{CDX}$	$\Delta\beta_1^{CDX}$	ΔI^{SPX}	$\Delta\beta_0^{SPX}$	ΔI^{CDX}	$\Delta\beta_0^{CDX}$	$\Delta\beta_1^{CDX}$	ΔI^{SPX}	$\Delta\beta_0^{SPX}$
$\Delta\beta_0^{CDX}$	0.56					0.40				
$\Delta\beta_1^{CDX}$	0.22	0.53				0.15	0.33			
ΔI^{SPX}	−0.79	−0.56	−0.28			−0.79	−0.62	−0.17		
$\Delta\beta_0^{SPX}$	0.67	0.62	0.31	−0.83		0.63	0.86	0.20	−0.81	
$\Delta\beta_1^{SPX}$	−0.55	−0.49	−0.33	0.62	−0.69	−0.56	−0.55	−0.30	0.68	−0.69

COVID-19 crisis, we report results both for the full sample (Panel A) and for an ex-COVID-19 sample that ends on December 31, 2019 (Panel B). For CDX, there is a highly positive correlation between changes in spread and volatility (0.62), which is consistent with the positively skewed implied volatility smiles. We also observe a somewhat weaker positive correlation between changes in spread and skewness (0.20), and a moderately positive correlation between changes in volatility and skewness (0.39). For SPX, the table confirms the well-known negative return-volatility correlation (−0.86), positive return-skewness correlation (0.74), and negative volatility-skewness correlation (−0.80). Regarding the cross-market interactions, we highlight the strongly negative correlation between CDX spread changes and SPX returns (−0.80), the highly positive correlation between volatility changes (0.69), and a somewhat more moderate negative correlation between skewness changes (−0.33). This correlation structure is robust to excluding the COVID-19 period.

III. A Structural Model for Pricing Index Options

We now propose a structural model to price credit and equity index options consistent with the debt and equity claims on each firm in the index. Asset value dynamics have a factor structure in which both idiosyncratic and systematic risk have a diffusive component and a jump component, and the common factor additionally features stochastic volatility and a variance-dependent jump intensity. Following Merton's (1974) seminal paper, we model each individual firm's CDS and equity as, respectively, a put option and a call option on the firm's asset value. To address the term structure of credit spreads, we allow outstanding debt to have different maturities as in Geske (1977), and we use the LHP approximation of Vasicek (1987) to model the index portfolios. Indexes and index options are given as compound options. In Section IV, we develop new results on multivariate transform analysis for affine processes to price these options analytically.

A. The Firms' Assets

We assume that each individual firm in the index has an asset value A_t^i that is driven by a common component A_t, which has stochastic volatility (ω_t) and is exposed to systematic Brownian (dW_t) and pure-jump (dN_t) shocks, and a firm-specific residual component, which is exposed to idiosyncratic Brownian (dW_t^i) and pure-jump (dN_t^i) shocks. Specifically, we assume that the risk-neutral asset value dynamics of (ex ante identical) individual firms are given by

$$\begin{aligned}
\frac{dA_t^i}{A_{t^-}^i} &= \frac{dA_t}{A_{t^-}} + \sigma_i dW_t^i + (e^{\gamma_i} - 1)dN_t^i - \lambda_i \nu_i dt \\
\frac{dA_t}{A_{t^-}} &= (r - \delta)dt + \sqrt{\omega_t} dW_t + (e^{\gamma} - 1)dN_t - \lambda_t \nu dt \\
d\omega_t &= \kappa(\bar{\omega} - \omega_t)dt + \sigma_{\omega}\sqrt{\omega_t}\left(\rho_{\omega} dW_t + \sqrt{1 - \rho_{\omega}{}^2} dZ_t\right),
\end{aligned}$$

where W_t^i, W_t, and Z_t are independent Brownian motions, N_t and N_t^i are independent Poisson counting processes with intensities $\lambda_t = \lambda_0 + \lambda_\omega \omega_t$ and λ_i, respectively, $\gamma \sim \mathcal{N}(m, v)$ and $\gamma_i \sim \mathcal{N}(m_i, v_i)$ are independent normal random variables, and we define $\nu = \mathbb{E}[e^{\gamma} - 1] = e^{m + \frac{v}{2}} - 1$ and $\nu_i = \mathbb{E}[e^{\gamma_i} - 1] = e^{m_i + \frac{v_i}{2}} - 1$. We assume that the firm pays continuous dividends, δA_t^i, to equity holders.

It is helpful to define $a_t^i = \log A_t^i$, $a_t = \log A_t$, and $\xi_t^i = a_t^i - a_t$, with ξ_t^i capturing firm-specific risk. The state vector

$$x_t = [a_t, \omega_t]^\top$$

captures the systematic risk components, whereas the relevant state vector when considering a specific firm can be defined as

$$x_t^i = \left[a_t, \omega_t, \xi_t^i\right]^\top .$$

The dynamics of these state variables are given in the Appendix, but here we note three properties that will be instrumental to deriving index option values: (i) both x_t and x_t^i are affine jump-diffusion processes (as defined in Duffie, Pan, and Singleton (2000)), (ii) $\forall i \;\; \xi_t^i$ are independent of x_t, and (iii) $\forall i \;\; a_T^i$ have i.i.d. distributions conditional on x_T.

B. The Firms' Debt

We consider a simplified debt structure with two outstanding zero-coupon bonds: a short-term bond with principal D_1 and maturity date T_1, and a long-term bond with principal D_2 and maturity date $T_2 > T_1$.[24] We assume that repayments of principals are made by equity holders, via "out-of-pocket" side payments, so that the asset value process is not affected.[25] Thus, equity holders will choose to default at T_1 if the continuation value from holding on to the equity is worth less than the principal payment D_1 they owe to debt holders at that time. This determines an endogenous default threshold, Φ_{T_1}, at T_1, where Φ_{T_1} is the asset value such that, right after D_1 has been paid by equity holders, the equity value equals D_1. At T_2, the default threshold is D_2, as in the standard Merton (1974) model. In case of default, we assume that a fraction α of assets is paid out to debt holders, while a fraction $1 - \alpha$ is lost because of bankruptcy costs. Finally, if the firm defaults at T_1, we assume that payments to debt holders are proportional to principal, so that holders of the short-term bond are paid a fraction $R_1 = \alpha \frac{D_1}{D_1 + D_2}$ of assets, while holders of the long-term bond are paid a fraction $R_2 = \alpha \frac{D_2}{D_1 + D_2}$.

C. Valuation of Bond, Equity, and CDS

Consider any firm i and let $t \leq T_1$. The value of the short-term bond is given by

$$B_t^{T_1,i} = e^{-r(T_1-t)} \left(D_1 \mathbb{E}_t \left[\mathbf{1}_{\left\{A_{T_1}^i \geq \Phi_{T_1}\right\}} \right] + \mathbb{E}_t \left[R_1 A_{T_1}^i \mathbf{1}_{\left\{A_{T_1}^i < \Phi_{T_1}\right\}} \right] \right),$$

where the first term is the present value of the bond's principle when it is repaid and the second term is the present value of the bond's recovery amount

[24] This is the simplest debt structure that allows us to get a term structure of credit spreads and generate variation in the risky annuity for long-term CDX contracts. The model can handle any number of bonds.

[25] This is a standard assumption in dynamic capital structure models (Black and Cox (1976), Leland (1994)).

when the firm defaults at T_1. The value of the long-term bond is given by

$$B_t^{T_2,i} = e^{-r(T_1-t)}\mathbb{E}_t\left[R_2 A_{T_1}^i \mathbf{1}_{\left\{A_{T_1}^i < \Phi_{T_1}\right\}}\right] + e^{-r(T_2-t)}\left(D_2\mathbb{E}_t\left[\mathbf{1}_{\left\{A_{T_1}^i \geq \Phi_{T_1}, A_{T_2}^i \geq D_2\right\}}\right] + \mathbb{E}_t\left[\alpha A_{T_2}^i \mathbf{1}_{\left\{A_{T_1}^i \geq \Phi_{T_1}, A_{T_2}^i < D_2\right\}}\right]\right),$$

where the first term is the present value of the bond's recovery amount when the firm defaults at T_1, and the second and third terms are, respectively, the present values of the bond's principle when it is repaid and the bond's recovery amount when the firm defaults at T_2, provided that the firm did not default at T_1.

The equity value is given by the asset value less the value of the two bonds and the present value of the expected bankruptcy costs, that is,

$$S_t^i = A_t^i - e^{-r(T_1-t)}\left(D_1\mathbb{E}_t\left[\mathbf{1}_{\left\{A_{T_1}^i \geq \Phi_{T_1}\right\}}\right] + \mathbb{E}_t\left[A_{T_1}^i \mathbf{1}_{\left\{A_{T_1}^i < \Phi_{T_1}\right\}}\right]\right) - e^{-r(T_2-t)}\left(D_2\mathbb{E}_t\left[\mathbf{1}_{\left\{A_{T_1}^i \geq \Phi_{T_1}, A_{T_2}^i \geq D_2\right\}}\right] + \mathbb{E}_t\left[A_{T_2}^i \mathbf{1}_{\left\{A_{T_1}^i \geq \Phi_{T_1}, A_{T_2}^i < D_2\right\}}\right]\right). \tag{3}$$

Consider a unit-notional CDS contract from t to T_2. The value of the protection leg is

$$V_t^{\text{Protection leg},i} = e^{-r(T_1-t)}\mathbb{E}_t\left[\left(1 - \frac{\alpha A_{T_1}^i}{D_1 + D_2}\right)\mathbf{1}_{\left\{A_{T_1}^i < \Phi_{T_1}\right\}}\right] + e^{-r(T_2-t)}\mathbb{E}_t\left[\left(1 - \frac{\alpha A_{T_2}^i}{D_2}\right)\mathbf{1}_{\left\{A_{T_1}^i \geq \Phi_{T_1}, A_{T_2}^i < D_2\right\}}\right],$$

where the first term is the present value of loss given default (LGD) at T_1 and the second term is the present value of LGD at T_2, provided that the firm did not default at T_1. The value of the premium leg with a coupon rate of C paid continuously is

$$V_t^{\text{Premium leg},i} = \left(\int_t^{T_1} e^{-r(u-t)}du + \int_{T_1}^{T_2} e^{-r(u-t)}du\,\mathbb{E}_t\left[\mathbf{1}_{\left\{A_{T_1}^i \geq \Phi_{T_1}\right\}}\right]\right) \times C,$$

where the coupon up to date T_1 always has to be paid because the firm cannot default before T_1 (the first term), whereas the coupon from T_1 to T_2 only has to be paid if the firm did not default at T_1 (the second term). Therefore, the upfront amount of the CDS contract is

$$\begin{aligned} U_t^i =& V_t^{\text{Protection leg},i} - V_t^{\text{Premium leg},i} \\ =& e^{-r(T_1-t)}\left((1 + C_1)\mathbb{E}_t\left[\mathbf{1}_{\left\{A_{T_1}^i < \Phi_{T_1}\right\}}\right] - \frac{\alpha}{D_1 + D_2}\mathbb{E}_t\left[A_{T_1}^i \mathbf{1}_{\left\{A_{T_1}^i < \Phi_{T_1}\right\}}\right] - C_1\right) \end{aligned}$$

$$+e^{-r(T_2-t)}\left(\mathbb{E}_t\left[\mathbf{1}_{\left\{A^i_{T_1}\geq\Phi_{T_1},A^i_{T_2}<D_2\right\}}\right]-\frac{\alpha}{D_2}\mathbb{E}_t\left[A^i_{T_2}\mathbf{1}_{\left\{A^i_{T_1}\geq\Phi_{T_1},A^i_{T_2}<D_2\right\}}\right]\right)-C_0, \tag{4}$$

where we have defined $C_0 = C\int_t^{T_1} e^{-r(u-t)}du$ and $C_1 = C\int_{T_1}^{T_2} e^{-r(u-T_1)}du$.

D. The Default Boundary at T_1

Valuation in the previous section depends on the default boundary at T_1. Note that after the payment of D_1 is made, the equity value becomes

$$S^i_{T_1}(a^i_{T_1},\omega_{T_1}) = A^i_{T_1} - e^{-r(T_2-T_1)}\left(D_2\mathbb{E}_{T_1}\left[\mathbf{1}_{\left\{A^i_{T_2}\geq D_2\right\}}\right]+\mathbb{E}_{T_1}\left[A^i_{T_2}\mathbf{1}_{\left\{A^i_{T_2}<D_2\right\}}\right]\right).$$

Therefore, the default boundary $\Phi(\omega)$, such that it is optimal to default at T_1 if $A^i_{T_1}\leq\Phi(\omega_{T_1})$, is given by the solution to the equation $S^i_{T_1}(\log\Phi(\omega),\omega) = D_1$. To obtain analytical valuations, we approximate the log-default boundary with an affine function:

$$\log\Phi(\omega)\approx\phi_0+\phi_1\omega. \tag{5}$$

We verify in Section V of the Internet Appendix that (5) is an accurate approximation.

E. Valuation of CDX and SPX

The upfront amount of the CDX is a simple average of the upfront amounts of the $N = 125$ single-name CDSs for the index constituents. Because N is large, we approximate the index upfront amount by letting $N\to\infty$. In this case, we obtain a simple analytical expression for the index upfront amount via the law of large numbers, which in turn allows us to price CDX options analytically. From (4), the index upfront amount, conditional on the common factors in x_t, is given by

$$\begin{aligned}
U_t(x_t) &= \lim_{N\to\infty}\frac{1}{N}\sum_{i=1}^{N}U^i_t \\
&= \mathbb{E}\left[U^i_t|x_t\right] \\
&= e^{-r(T_1-t)}\left((1+C_1)\mathbb{E}\left[\mathbf{1}_{\left\{A^i_{T_1}<\Phi(\omega_{T_1})\right\}}|x_t\right]-\frac{\alpha}{D_1+D_2}\mathbb{E}\left[A^i_{T_1}\mathbf{1}_{\left\{A^i_{T_1}<\Phi(\omega_{T_1})\right\}}|x_t\right]-C_1\right) \\
&\quad+e^{-r(T_2-t)}\left(\mathbb{E}\left[\mathbf{1}_{\left\{A^i_{T_1}\geq\Phi(\omega_{T_1}),A^i_{T_2}<D_2\right\}}|x_t\right]-\frac{\alpha}{D_2}\mathbb{E}\left[A^i_{T_2}\mathbf{1}_{\left\{A^i_{T_1}\geq\Phi(\omega_{T_1}),A^i_{T_2}<D_2\right\}}|x_t\right]\right)-C_0.
\end{aligned}$$

Similarly, from (3), the value of the SPX is given by

$$
\begin{aligned}
S_t(x_t) &= \lim_{N\to\infty}\frac{1}{N}\sum_{i=1}^{N} S_t^i \\
&= \mathbb{E}\left[S_t^i | x_t\right] \\
&= A_t - e^{-r(T_1-t)}\left(D_1\mathbb{E}\left[\mathbf{1}_{\left\{A^i_{T_1}\geq\Phi(\omega_{T_1})\right\}}|x_t\right] + \mathbb{E}\left[A^i_{T_1}\mathbf{1}_{\left\{A^i_{T_1}<\Phi(\omega_{T_1})\right\}}|x_t\right]\right) \\
&\quad -e^{-r(T_2-t)}\left(D_2\mathbb{E}\left[\mathbf{1}_{\left\{A^i_{T_1}\geq\Phi(\omega_{T_1}),A^i_{T_2}\geq D_2\right\}}|x_t\right] + \mathbb{E}\left[A^i_{T_2}\mathbf{1}_{\left\{A^i_{T_1}\geq\Phi(\omega_{T_1}),A^i_{T_2}<D_2\right\}}|x_t\right]\right).
\end{aligned}
$$

F. Valuation of CDX and SPX Options

Using the notation $\mathbb{E}_0[\cdot] := \mathbb{E}[\cdot\,|\,x_0]$, the time-0 value of a CDX call option with strike K and expiration at T_0 is

$$
\begin{aligned}
C_0^{CDX} &= e^{-rT_0}\mathbb{E}_0\left[\max(U_{T_0}(x_{T_0}) - K, 0)\right] \\
&= e^{-rT_0}\mathbb{E}_0\left[(U_{T_0}(x_{T_0}) - K)\mathbf{1}_{\left\{A_{T_0}<\underline{A}(\omega_{T_0})\right\}}\right] \\
&= e^{-rT_1}\left((1+C_1)\mathbb{E}_0\left[\mathbf{1}_{\left\{A_{T_0}<\underline{A}(\omega_{T_0}),A^i_{T_1}<\Phi(\omega_{T_1})\right\}}\right] - \frac{\alpha}{D_1+D_2}\mathbb{E}_0\left[A^i_{T_1}\mathbf{1}_{\left\{A_{T_0}<\underline{A}(\omega_{T_0}),A^i_{T_1}<\Phi(\omega_{T_1})\right\}}\right]\right) \\
&\quad + e^{-rT_2}\left(\mathbb{E}_0\left[\mathbf{1}_{\left\{A_{T_0}<\underline{A}(\omega_{T_0}),A^i_{T_1}\geq\Phi(\omega_{T_1}),A^i_{T_2}<D_2\right\}}\right] - \frac{\alpha}{D_2}\mathbb{E}_0\left[A^i_{T_2}\mathbf{1}_{\left\{A_{T_0}<\underline{A}(\omega_{T_0}),A^i_{T_1}\geq\Phi(\omega_{T_1}),A^i_{T_2}<D_2\right\}}\right]\right) \\
&\quad - e^{-rT_0}\tilde{K}\mathbb{E}_0\left[\mathbf{1}_{\left\{A_{T_0}<\underline{A}(\omega_{T_0})\right\}}\right],
\end{aligned}
$$

where $\tilde{K} = K + C_0 + C_1 e^{-r(T_1-T_0)}$ and $\underline{a}(\omega) = \log\underline{A}(\omega)$ is the exercise boundary, implicitly defined by the equation $U_{T_0}(\underline{a}(\omega), \omega) = K$, such that it is optimal to exercise the CDX call at T_0 when $a_{T_0} \leq \underline{a}(\omega_{T_0})$. To value CDX options analytically, we approximate the exercise boundary with an affine function:

$$
\underline{a}(\omega) = \underline{a}_0 + \underline{a}_1\omega. \tag{6}
$$

Similarly, the time-0 value of an SPX call option with strike K and expiration at T_0 is

$$
\begin{aligned}
C_0^{SPX} &= e^{-rT_0}\mathbb{E}_0\left[\max(S_{T_0}(x_{T_0}) - K, 0)\right] \\
&= e^{-rT_0}\mathbb{E}_0\left[(S_{T_0}(x_{T_0}) - K)\mathbf{1}_{\left\{A_{T_0}\geq\overline{A}(\omega_{T_0})\right\}}\right]
\end{aligned}
$$

$$
\begin{aligned}
&= e^{-rT_0}\mathbb{E}_0\left[A_{T_0}\mathbf{1}_{\left\{A_{T_0}\geq\overline{A}(\omega_{T_0})\right\}}\right]\\
&\quad - e^{-rT_1}\left(D_1\mathbb{E}_0\left[\mathbf{1}_{\left\{A_{T_0}\geq\overline{A}(\omega_{T_0}),A^i_{T_1}\geq\Phi(\omega_{T_1})\right\}}\right]+\mathbb{E}_0\left[A^i_{T_1}\mathbf{1}_{\left\{A_{T_0}\geq\overline{A}(\omega_{T_0}),A^i_{T_1}<\Phi(\omega_{T_1})\right\}}\right]\right)\\
&\quad - e^{-rT_2}\left(D_2\mathbb{E}_0\left[\mathbf{1}_{\left\{A_{T_0}\geq\overline{A}(\omega_{T_0}),A^i_{T_1}\geq\Phi(\omega_{T_1}),A^i_{T_2}\geq D_2\right\}}\right]+\mathbb{E}_0\left[A^i_{T_2}\mathbf{1}_{\left\{A_{T_0}\geq\overline{A}(\omega_{T_0}),A^i_{T_1}\geq\Phi(\omega_{T_1}),A^i_{T_2}<D_2\right\}}\right]\right)\\
&\quad - e^{-rT_0}K\mathbb{E}_0\left[\mathbf{1}_{\left\{A_{T_0}\geq\overline{A}(\omega_{T_0})\right\}}\right],
\end{aligned}
$$

where $\overline{a}(\omega)=\log\overline{A}(\omega)$ is the exercise boundary, implicitly defined by the equation $S_{T_0}(\overline{a}(\omega),\omega)=K$, such that it is optimal to exercise the SPX call at T_0 if $a_{T_0}\geq\overline{a}(\omega_{T_0})$. To value SPX options analytically, we approximate the exercise boundary with an affine function:

$$\overline{a}(\omega)=\overline{a}_0+\overline{a}_1\omega. \tag{7}$$

We verify in Section V of the Internet Appendix that (6) and (7) are accurate approximations to the respective exercise boundaries.

IV. Multivariate Transform Analysis for Affine Processes

The valuation of indexes and index options described above can be reduced to computing the following *generalized affine transform*:

$$G^{\alpha}_{\beta}(y_1,\ldots,y_n;\overline{X}_{T_0},\boldsymbol{T})=\mathbb{E}\left[e^{\alpha\cdot X_{T_n}}\mathbf{1}_{\left\{\beta_1\cdot X_{T_1}\leq y_1,\ldots,\beta_n\cdot X_{T_n}\leq y_n\right\}}\,|\overline{X}_{T_0}\right] \tag{8}$$

defined for an N-dimensional affine state vector X_t with a subvector $\overline{X}_t$ (i.e., $X_t=[\begin{smallmatrix}\overline{X}_t\\ \underline{X}_t\end{smallmatrix}]$), a vector $\boldsymbol{T}=[T_0,\ldots,T_n]$ of increasing dates, an (N,n)-matrix $\boldsymbol{\beta}$ with column vectors β_i (i.e., $\boldsymbol{\beta}=[\beta_1,\ldots,\beta_n]$), and an N-vector α.

This is a multivariate extension of the generalized affine transform presented in the classic paper by Duffie, Pan, and Singleton (2000), who consider the case with $n=1$ and $\overline{X}_t=X_t$, and use it to value standard derivatives, such as European call and put options, written on an underlying with N-dimensional affine dynamics.

The multivariate case that we present here is useful to value more complex derivatives with payoffs involving multiple dates, such as compound options and cliquet options, or payoffs that depend on several underlyings, such as outperformance options or basket options.

Duffie, Pan, and Singleton (2000) obtain the univariate solution using the Fourier inversion theorem of Gil-Pelaez (1951). Here, we follow a similar approach by relying on the multidimensional version of that theorem derived in Shephard (1991).

To solve the generalized affine transform, we first rewrite (where, to simplify notation, we drop the dependence on $\boldsymbol{T}$)

$$G^{\alpha}_{\boldsymbol{\beta}}(y_1,\ldots,y_n;\,\overline{X}_{T_0}) = \mathbb{E}\left[e^{\alpha\cdot X_{T_n}}\,|\overline{X}_{T_0}\right]\,\mathbb{E}^{\alpha}\left[\mathbf{1}_{\left\{\beta_1\cdot X_{T_1}\le y_1,\ldots,\beta_n\cdot X_{T_n}\le y_n\right\}}\,|\overline{X}_{T_0}\right]$$
$$:= \Psi(\alpha;\overline{X}_{T_0},T_0,T_n)\,G^{\alpha}_{\boldsymbol{\beta}}(y_1,\ldots,y_n;\,\overline{X}_{T_0}), \tag{9}$$

where, for some n-dimensional parameter vector α,

$$\Psi(\alpha;\overline{X}_{T_0},T_0,T) := \mathbb{E}\left[e^{\alpha\cdot X_T}\,|\overline{X}_{T_0}\right] \tag{10}$$

is the moment-generating function of X_T conditional on the subvector $\overline{X}_{T_0}$, which in general need not have an exponential affine solution. Instead, the classic exponential affine moment-generating function that defines the affine process X_t is[26]

$$\Psi(\alpha;X_{T_0},T_0,T) := \mathbb{E}\left[e^{\alpha\cdot X_T}\,|X_{T_0}\right] \tag{11}$$

$$= e^{b_\alpha(T_0,T)+c_\alpha(T_0,T)\cdot X_{T_0}}, \tag{12}$$

where $b_\alpha(T_0,T)$ and $c_\alpha(T_0,T)$ are deterministic functions.[27]

Note that $G^{\alpha}_{\boldsymbol{\beta}}(y_1,\ldots,y_n;\,\overline{X}_{T_0}) \equiv \mathbb{P}^{\alpha}(\beta_i\cdot X_{T_i}\le y_i\ \forall i=1,\ldots,n)$ is the multivariate cumulative distribution function (conditional on $T_0,\overline{X}_{T_0}$) of the n random variables $x_i=\beta_i\cdot X_{T_i},\ \ i=1,\ldots,n$ under the probability measure $\mathbb{P}^{\alpha}$ defined by

$$\frac{d\mathbb{P}^{\alpha}}{d\mathbb{P}} = \frac{e^{\alpha\cdot X_{T_n}}}{\Psi(\alpha;\overline{X}_{T_0},T_0,T_n)}.$$

We then obtain the following theorem from multivariate Fourier inversion.

THEOREM 1: *Define*

$$\begin{aligned}U(y_1,\ldots,y_n) &= 2^n G^{\alpha}_{\{\beta_1,\ldots,\beta_n\}}(y_1,\ldots,y_n)\\ &\quad - 2^{n-1}\Big[G^{\alpha}_{\{\beta_2,\ldots,\beta_n\}}(y_2,\ldots,y_n)+\cdots+G^{\alpha}_{\{\beta_1,\ldots,\beta_{n-1}\}}(y_1,\ldots,y_{n-1})\Big]\\ &\quad + 2^{n-2}\Big[G^{\alpha}_{\{\beta_3,\ldots,\beta_n\}}(y_3,\ldots,y_n)+\cdots+G^{\alpha}_{\{\beta_1,\ldots,\beta_{n-2}\}}(y_1,\ldots,y_{n-2})\Big]\\ &\quad + \cdots + (-1)^n.\end{aligned}$$

Then if n is odd we have

$U(y_1,\ldots,y_n) =$

[26] We note the slight abuse of notation: $\Psi(\beta;X,t,T)$ and $\Psi(\beta;\overline{X},t,T)$ are different functions. We hope this leads to no confusion as the two vectors X and $\overline{X}$ have different sizes.

[27] These functions are related to the generator of the affine process via a system of ordinary differential equations; see Duffie, Filipović, and Schachermayer (2003).

$$\frac{(-2)^n}{(2\pi)^n}\int_0^\infty \cdots \int_0^\infty 2\mathrm{i}^{n-1} \underset{u_2}{\Delta} \cdots \underset{u_n}{\Delta} Im\left[\frac{e^{-\mathrm{i}u\cdot y}\Psi^\alpha(\mathrm{i}u_1\beta_1,\ldots,\mathrm{i}u_n\beta_n;\overline{X}_{T_0},T_0,T_1,\ldots,T_n)}{u_1\ldots u_n}\right]du_1\ldots du_n,$$

and if n is even we have

$$U(y_1,\ldots,y_n)=$$

$$\frac{(-2)^n}{(2\pi)^n}\int_0^\infty \cdots \int_0^\infty 2\mathrm{i}^{n} \underset{u_2}{\Delta} \cdots \underset{u_n}{\Delta} Re\left[\frac{e^{-\mathrm{i}u\cdot y}\Psi^\alpha(\mathrm{i}u_1\beta_1,\ldots,\mathrm{i}u_n\beta_n;\overline{X}_{T_0},T_0,T_1,\ldots,T_n)}{u_1\ldots u_n}\right]du_1\ldots du_n,$$

where for $1 \leq j \leq n$ *and* $f : \mathbb{R}^n \to \mathbb{R}$*, the operator* $\underset{u_j}{\Delta}$ *is defined by*

$$\underset{u_j}{\Delta} f(u) = f(u_1,\ldots,u_{j-1},u_j,u_{j+1},\ldots,u_n) + f(u_1,\ldots,u_{j-1},-u_j,u_{j+1},\ldots,u_n),$$

and for all $j \geq 1$

$$\Psi^\alpha(\beta_1,\ldots,\beta_j;\overline{X}_{T_0},T_0,T_1,\ldots,T_j)=\frac{\Psi(\beta_1,\ldots,\beta_{j-1},\beta_j+\alpha;\overline{X}_{T_0},T_0,T_1,\ldots,T_j)}{\Psi(\alpha;\overline{X}_{T_0},T_0,T_j)}.$$

For $j = 1$*, the conditional moment-generating function is defined in (10), and for all* $j > 1$ *we define recursively*

$$\begin{aligned}\Psi(\beta_1,\ldots,\beta_j;&\overline{X}_{T_0},T_0,T_1,\ldots,T_j)\\ &=\Psi(\beta_1,\ldots,\beta_{j-2},\beta_{j-1}+c_{\beta_j}(T_{j-1},T_j);\overline{X}_{T_0},T_0,T_1,\ldots,T_{j-1})e^{b_{\beta_j}(T_{j-1},T_j)}.\end{aligned}$$

PROOF: See the Appendix. □

Note that for $n = 1$ our theorem recovers the transform inversion formula of Duffie, Pan, and Singleton (2000, proposition 2).

COROLLARY 1: *Using Theorem 1 in the definition (9) for the case* $n = 1$ *and with* $\overline{X}_t = X_t$*, we obtain*

$$G^\alpha_{\beta_1}(y_1;X_{T_0},T_0,T_1)=\frac{\Psi(\alpha;X_{T_0},T_0,T_1)}{2}-\frac{1}{\pi}\int_0^\infty Im\left[\frac{e^{-\mathrm{i}u_1y_1}\Psi(\alpha+\mathrm{i}u_1\beta_1;X_{T_0},T_0,T_1)}{u_1}\right]du_1.$$

All indexes and index options are valued with Theorem 1 applied to the three-dimensional affine process $X_t = x^i_t$, using as subvector either $\overline{X}_t = x_t$ or $\overline{X}_t = x^i_t$ (Section IV of the Internet Appendix shows how all expectations in the pricing formulas in Section III can be expressed in terms of the generalized transform (8)). For this purpose, in the next theorem we present closed-form solutions to the two moment-generating functions (10) and (11). While the exponential affine solution in (12) is standard, an exponential affine solution to (10) does not automatically follow, and indeed obtains here only because when considering the affine process $x^i_t = [\begin{smallmatrix} x_t \\ \xi^i_t \end{smallmatrix}]$, the subvector process x_t is independent of ξ^i_t.

THEOREM 2: *For the affine process $X_t := x_t^i$, we obtain, for conditioning subvectors, respectively, given by (i) $\overline{X}_t = x_t^i$ and (ii) $\overline{X}_t = x_t$,*

$$(i)\ \ \Psi(\beta; x_t^i, t, T) := \mathbb{E}\left[e^{\beta\cdot x_T^i}\,|\,x_t^i\right] = e^{b_\beta(t,T)+c_\beta(t,T)\cdot x_t^i},$$

$$(ii)\ \ \Psi(\beta; x_t, t, T) := \mathbb{E}\left[e^{\beta\cdot x_T^i}\,|\,x_t\right] = e^{\zeta(\beta_3)T+B(T-t;\beta_1,\beta_2)+\beta_1 a_t+C(T-t;\beta_1,\beta_2)\omega_t},$$

where $\beta = [\beta_1, \beta_2, \beta_3]^\top$ is a vector of parameters and

$$b_\beta(t, T) = \zeta(\beta_3)(T-t) + B(T-t; \beta_1, \beta_2),$$

$$c_\beta(t, T) = \begin{bmatrix} \beta_1 \\ C(T-t; \beta_1, \beta_2) \\ \beta_3 \end{bmatrix},$$

where the functions $\zeta(\beta_3)$, $B(T-t; \beta_1, \beta_2)$, and $C(T-t; \beta_1, \beta_2)$ have closed-form solutions given in equations (A.4), (A.5), and (A.6).

PROOF: See the Appendix. □

V. The Relative Pricing of Index Options

A. Calibration Procedure

The main empirical analysis consists of fitting the model to the CDX term structure, the SPX level, and the SPX option surface, and then price the CDX option surface out-of-sample. As a robustness check, we also conduct the reverse exercise, fitting to the CDX option surface and pricing the SPX option surface out-of-sample. In particular, we force a perfect fit to the 1Y and 5Y CDX and the SPX level (as well as the SPX dividend yield and the short-term and long-term index leverage ratios), and minimize the sum of squared pricing errors for index options.[28] It is especially important to price the 5Y CDX and the SPX level accurately as otherwise it is difficult to interpret option pricing errors.

As in Collin-Dufresne, Goldstein, and Yang (2012), the parameters governing the dynamics of the common factors are held fixed for each six-month period over which a CDX series is on-the-run. The common factors and the remaining parameters change from each observation date to the next. As in Section II, we use weekly data. Additional details on the estimation are given in Section VII of the Internet Appendix.

Some parameters are fixed ex ante (we have verified that our results are robust to reasonable variations in these parameters). First, we set $m_i = -5$ and $v_i = 0$, implying that an idiosyncratic jump leads to almost certain default

[28] See Section VIII of the Internet Appendix for details on the computation of the index leverage ratios using Compustat data. The SPX dividend yield is obtained from the put-call parity relation for SPX options.

Table IV

Parameter Estimates

The table reports the sample mean and sample standard deviation of the calibrated parameters (for ease of interpretation, the table reports statistics for D_1/A_t and D_2/A_t instead of D_1 and D_2). A number of model parameters are fixed in advance: $m_i = -5$, $v_i = 0$, $\alpha = 0.8$, $\sigma_\omega = 0.20$, and $\rho_\omega = -0.70$. The sample period is February 29, 2012 to April 29, 2020 (427 weekly observations).

	ω_t	κ	$\bar{\omega}$	λ_0	λ_ω	m	$\sqrt{v}$	A_t	σ_i	λ_i	D_1/A_t	D_2/A_t	δ
Panel A: Calibration to SPX Options													
Mean	0.0101	1.074	0.0310	0.000	8.33	−0.171	0.160	2905.8	0.284	0.001	0.034	0.227	0.015
St. dev.	0.0065	0.831	0.0126	0.000	5.32	0.052	0.030	689.5	0.039	0.001	0.003	0.014	0.003
Panel B: Calibration to CDX Options													
Mean	0.0185	1.751	0.0247	0.021	63.96	−0.045	0.167	2905.8	0.212	0.001	0.034	0.227	0.015
St. dev.	0.0179	0.914	0.0089	0.129	39.33	0.038	0.027	689.6	0.073	0.001	0.003	0.014	0.003

for a company, and calibrate only the idiosyncratic jump intensity.[29] Second, bankruptcy costs are set to 20%, corresponding to $\alpha = 0.80$, which is roughly in line with empirical estimates (see, e.g., Andrade and Kaplan (1998) and Davydenko, Strebulaev, and Zhao (2012)). Third, the risk-free interest rate is set to the two-month rate from the bootstrapped LIBOR/swap curve. Fourth, in the common factor dynamics, the parameters σ_ω and ρ_ω are invariant under a change of measure. In the context of calibrating stochastic-volatility jump-diffusion models to equity index options, Broadie, Chernov, and Johannes (2007) stress the importance of *time-series consistency*, i.e., restricting those parameters that are invariant under a change of measure to their values under the physical measure. In Section VII of the Internet Appendix, we show that setting $\sigma_\omega = 0.20$ and $\rho_\omega = -0.70$ makes the corresponding vol-of-vol and correlation parameters for SPX returns largely consistent with recent time-series studies. We verify ex post that similar values for σ_ω and ρ_ω are obtained from the time series of the calibrated factors.

B. Results

Table IV reports the sample mean and sample standard deviation of the calibrated parameters, with Panels A and B showing results when calibrating to SPX and CDX options, respectively.[30] In both cases, there is strong evidence for stochastic volatility and variance-dependent jump intensities (while λ_0 is

[29] The total expected loss due to idiosyncratic jumps is essentially pinned down by the 1Y CDX, which is effectively a deep OTM put option on firm assets. However, we found it difficult to separately identify idiosyncratic jump intensity and jump size parameters.

[30] Tables IA.I and IA.II in the Internet Appendix report parameter estimates for each time period over which a CDX series is on-the-run.

estimated to be close to zero).[31] It is instructive to compare the two sets of estimates in terms of the implications for the unconditional systematic and total asset volatility ($\sqrt{\bar{\omega}+\lambda(m^2+v)}$ and $\sqrt{\bar{\omega}+\sigma_i^2+\lambda(m^2+v)+\lambda_i(m_i^2+v_i)}$, respectively, where $\lambda=\lambda_0+\lambda_\omega\bar{\omega}$), and the resulting unconditional correlation between firm asset values. The underlying indexes depend on total asset risk, and given that we always calibrate to the index levels, it is unsurprising that total asset volatility is very similar across the two calibrations (0.39 vs. 0.38). Index options, in contrast, depend largely on systematic asset risk, which can differ across the two calibrations. Indeed, systematic asset volatility is lower when calibrating to SPX options than when calibrating to CDX options (0.21 vs. 0.27). Consequently, the asset correlation implied from SPX options is lower than implied from CDX options (0.30 vs. 0.51).[32] This provides the first indication that the model will not match both sets of index options simultaneously; we can expect that calibrating to SPX options will tend to underprice CDX options while calibrating to CDX options will tend to overprice SPX options.

To assess the fit to options, on each observation date we compute the mean pricing error (ME) and root mean squared pricing error (RMSE) across each option surface, where pricing errors are given as the relative difference between fitted and actual implied volatilities, $\frac{\hat{\sigma}^{IV}-\sigma^{IV}}{\sigma^{IV}}$. Table V reports the sample means of the resulting ME and RMSE time series. Consider first the results when calibrating to SPX options. The in-sample fit is very good, with an average ME of essentially zero and not statistically significant. In contrast, the out-of-sample fit to CDX options produces an average ME of −0.283, which is highly statistically significant (that the out-of-sample CDX RMSE is larger than the in-sample SPX RMSE is to be expected). That is, as alluded to above, fitted CDX option prices are, on average, lower than market prices.

Consider next the results when calibrating to CDX options. These are the mirror image of the previous results. The in-sample fit to CDX options is very good, with an insignificant average ME, while the out-of-sample fit to SPX options has an average ME of 0.49, which again is highly statistically significant.

Figure 4 shows the time series of the out-of-sample ME for CDX options when calibrating to SPX options (blue line) and the out-of-sample ME for SPX options when calibrating to CDX options (red line). The two lines almost

[31] We verify that values of σ_ω and ρ_ω obtained from the time series of the calibrated factors are consistent with their ex ante predetermined values. We estimate σ_ω as the standard deviation of $\frac{\omega_{t+1}-\omega_t}{\sqrt{\omega_t}}$ times $\sqrt{52}$ and ρ_ω as the correlation between $\frac{\log A_{t+1}-\log A_t}{\sqrt{\omega_t}}$ and $\frac{\omega_{t+1}-\omega_t}{\sqrt{\omega_t}}$. For the ex-COVID-19 sample, we get $\sigma_\omega=0.21$ and $\rho_\omega=-0.77$ when calibrating to SPX options, and $\sigma_\omega=0.25$ and $\rho_\omega=-0.55$ when calibrating to CDX options, which are roughly in line with the predetermined values. Including the COVID-19 period leads to slightly higher estimates of σ_ω.

[32] To put these correlations into perspective, we directly compute pairwise correlations of daily asset returns among index constituents per calendar quarter, and then average across quarters (see Section XII of the Internet Appendix for details on the computation of asset returns). We require each return time series to comprise at least 50 daily returns in the respective quarter. The average pairwise asset correlations are remarkably similar for the two indexes, 0.29 for SPX and 0.28 for CDX. The extent to which risk-neutral correlations inferred from index options exceed physical correlations depends, particularly in the presence of jumps, on risk premia and is beyond the scope of this paper.

Table V

Pricing Errors

On each observation date, we compute the mean pricing error (ME) and root mean squared pricing error (RMSE) for SPX options and CDX options, where pricing errors are given as the relative difference between fitted and actual implied volatilities. The table reports sample means of the resulting ME and RMSE time series. In parentheses are t-statistics corrected for heteroskedasticity and serial correlation up to 52 lags using the approach of Newey and West (1987). The full sample period is February 29, 2012 to April 29, 2020 (427 weekly observations). The ex-COVID-19 sample period is February 29, 2012 to December 31, 2019 (410 weekly observations).

	SPX Options		CDX Options	
Calibrated to	ME	RMSE	ME	RMSE
Panel A: Full Sample				
SPX Options	−0.003	0.085	−0.283	0.296
	(−0.66)		(−12.47)	
CDX Options	0.493	0.590	−0.003	0.033
	(16.74)		(−1.56)	
Panel B: Ex-COVID-19 Sample				
SPX Options	−0.002	0.085	−0.289	0.301
	(−0.48)		(−13.01)	
CDX Options	0.500	0.596	−0.003	0.031
	(17.04)		(−1.69)	

always have opposite sign and they are highly negatively correlated (correlation coefficient of −0.81), so that if the mispricing worsens according to one calibration, it usually also does so according to the other, confirming the robustness of the results. We note that there is a tendency for the mispricing to decrease over time.

To further investigate model performance, we focus on the version calibrated to SPX options. First, we investigate which dimensions of the CDX option surface the model has difficulty matching. To do so, we run the regression (2) on the fitted implied volatilities and measure the model fit in terms of how close the β-estimates obtained from the fitted data are to the original β-estimates. In Figure 3, the red lines show the β-estimates from the fitted data. The figure confirms the model's accurate (in-sample) fit to SPX options in terms of both volatility (middle-right panel) and skewness (lower-right panel). The figure also shows that the model has a relatively accurate (out-of-sample) fit to CDX skewness (lower-left panel). However, the figure shows that the model has a poor (out-of-sample) fit to CDX volatility. While the model appears to capture the variation in volatility relatively well, the level of model-implied volatility is consistently lower than the market. Indeed, the sample means of β_0^{CDX} in the data and the fitted data are 0.47 and 0.33, respectively.

Next, we investigate the extent to which the model captures the index-volatility-skewness correlation structure discussed in Section II. The correlations computed from the fitted data are reported in the right part of Table III.

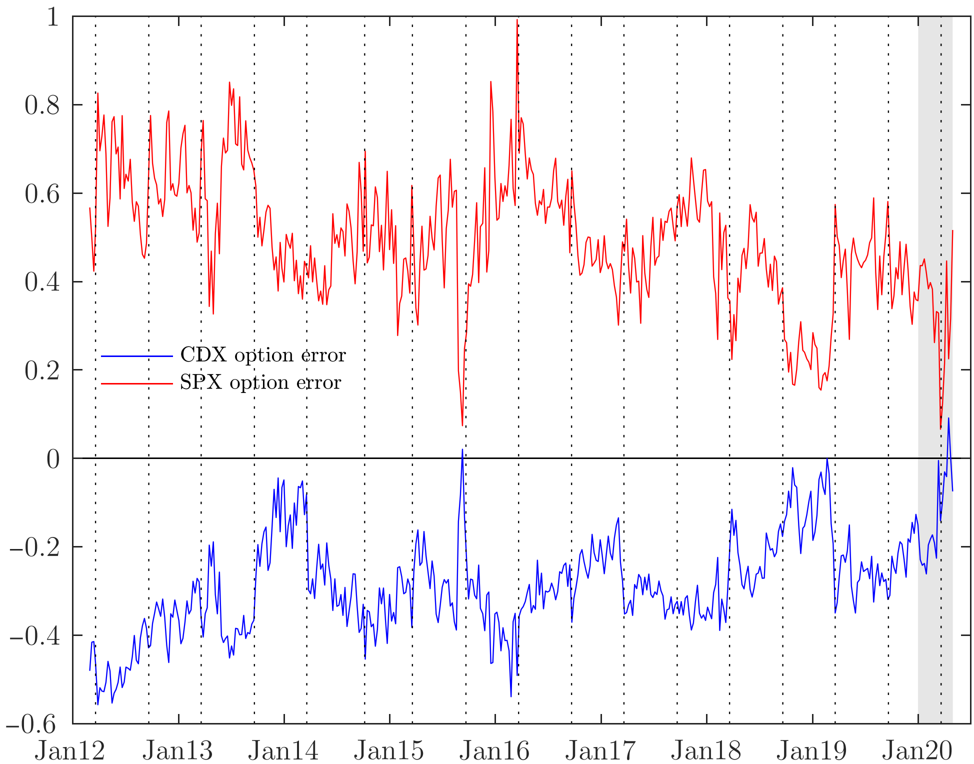

Figure 4. Out-of-sample fit to CDX and SPX options. On each observation date, we compute the mean out-of-sample pricing error (ME), i.e., for the model calibrated to SPX options, we compute the pricing error for CDX options (blue line), and for the model calibrated to CDX options, we compute the pricing error for SPX options (red line). Pricing errors are given as the relative difference between fitted and actual implied volatilities. Vertical dotted lines mark CDX roll dates. The sample period is February 29, 2012 to April 29, 2020 (427 weekly observations). The shaded area marks the COVID-19 period starting on January 1, 2020.

Within the SPX market, there is a close (in-sample) match to the data. More importantly, within the CDX market, there is a relatively good (out-of-sample) match to the correlation between spread and volatility (0.49 vs. 0.62 in the data), but somewhat too low correlations between volatility and skewness (0.11 vs. 0.20 in the data) and between spread and skewness (0.22 vs. 0.39 in the data). Regarding the cross-market interactions, the model largely captures the correlations between SPX and CDX volatility (0.83 vs. 0.69 in the data) and between SPX and CDX skewness (−0.25 vs. −0.33 in the data) as well as the remaining "off-diagonal" correlations.[33] These findings hold true in the ex-COVID-19 sample.

[33] Note that by design of the estimation procedure, the correlation between SPX returns and CDX spread changes is matched exactly.

To summarize, the model captures many aspects of the joint dynamics of the credit and equity index options data. However, it is not able to capture the relative levels of CDX and SPX option prices. In particular, calibrating the model to the SPX implied volatility surface produces a CDX implied volatility surface that, while having largely the correct shape, is consistently below the market.

C. Understanding the Sources of Volatilities and Smiles

In the model, index volatility is driven by several sources, namely, the financial leverage effect as well as stochastic volatility and jumps in the systematic asset factor. Let I_t denote the index (either the SPX level or the CDX spread), in which case the instantaneous variance of index returns is given as

$$\underbrace{\left(\frac{\partial I_t}{\partial A_t}\frac{A_t}{I_t}\right)^2\omega_t}_{\text{Financial leverage}} + \underbrace{\left(\frac{\partial I_t}{\partial \omega_t}\frac{1}{I_t}\sigma_\omega\right)^2\omega_t}_{\text{Stochastic asset vol}} + \underbrace{2\frac{\partial I_t}{\partial A_t}\frac{\partial I_t}{\partial \omega_t}\frac{A_t}{I_t^2}\sigma_\omega\rho_\omega\omega_t}_{\text{Covariance}} + \underbrace{\lambda_t\mathbb{E}\left[\left(\frac{I(A_{t-}e^\gamma,\omega_t)}{I(A_{t-},\omega_t)}-1\right)^2\right]}_{\text{Jumps}}. \tag{13}$$

To provide intuition about the model, in this section we show how these different elements affect both the relative levels of index volatility as well as the shapes of the index implied volatility smiles. For the sake of illustration, we focus on two-month options.

We start from the parameter estimates from Panel A in Table IV. The instantaneous volatility of simple returns on the systematic asset factor, $\sqrt{\omega_t + \lambda_t\mathbb{E}[(e^\gamma - 1)^2]}$, is 0.116. We consider four versions of the model that all have this systematic asset volatility but differ in terms of its sources. For each version of the model, we recalibrate A_t, σ_i, λ_i, D_1, D_2, and δ to the sample means of the 1Y and 5Y CDX upfronts, the SPX level, the SPX dividend yield, and the index leverage ratios, so that these quantities are held constant across versions.

First, as a natural benchmark, we consider a version with deterministic diffusive volatility ($\omega_t = 0.0135$, $\sigma_\omega = \rho_\omega = \lambda_0 = \lambda_\omega = 0$), in which case only the financial leverage effect is present. The instantaneous volatilities of CDX and SPX returns are 0.151 and 0.245, respectively, giving an *index volatility ratio* of 1.62. Figure 5 (blue lines) shows the implied volatility smiles. Both curves are quite flat, and in striking contrast to the data, the CDX implied volatility smile exhibits a negative slope.[34]

Second, we turn on stochastic asset volatility, but with zero correlation between asset returns and volatility ($\omega_t = 0.0135$, $\sigma_\omega = 0.2$, $\rho_\omega = \lambda_0 = \lambda_\omega = 0$). This adds the second term in (13), which originates from the fact that the index value depends directly on ω_t. However, this term is greater for CDX than SPX (we can think of the CDX and SPX as, respectively, a deep OTM and in-the-money option on the asset value, so that in relative terms CDX is more

[34] In Section IX of the Internet Appendix, we prove analytically that in the classic Merton (1974) model the leverage effect generates a negative implied volatility skew for both credit and equity options.

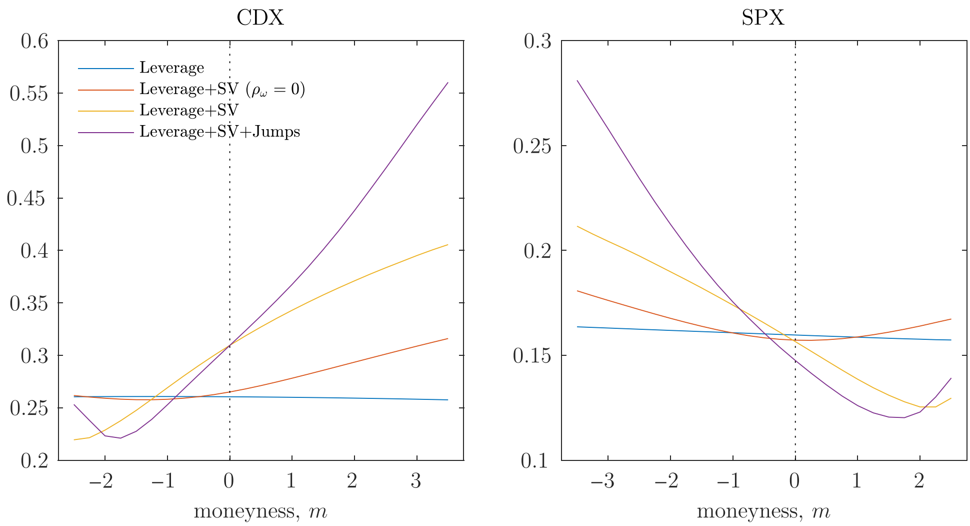

Figure 5. Sources of implied volatility smiles. The figure shows how the financial leverage effect and stochastic volatility (SV) and jumps in the systematic asset factor affect the implied volatility smiles for CDX and SPX options with a two-month maturity. The first model version (blue lines) has deterministic systematic asset volatility ($\omega_t = 0.0135, \sigma_\omega = \rho_\omega = \lambda_0 = \lambda_\omega = 0$) and the smiles are due only to the financial leverage effect. The second version (red lines) adds SV, but with zero correlation between asset returns and volatility ($\omega_t = 0.0135, \sigma_\omega = 0.2, \rho_\omega = \lambda_0 = \lambda_\omega = 0$). The third version (yellow lines) adds negative correlation between asset returns and volatility ($\omega_t = 0.0135, \sigma_\omega = 0.2, \rho_\omega = -0.70, \lambda_0 = \lambda_\omega = 0$). The fourth version (purple lines) adds jumps ($\omega_t = 0.0101, \sigma_\omega = 0.2, \rho_\omega = -0.70, \lambda_0 = 0.000, \lambda_\omega = 8.33, m = -0.171, \sqrt{v} = 0.160$). All versions of the model have the same instantaneous volatility of the systematic asset factor. For each model version, A_t, σ_i, λ_i, D_1, D_2, and δ are calibrated to match the sample means of 1Y and 5Y CDX upfronts, the SPX level, the SPX dividend yield, and the index leverage ratios. The remaining parameters are given in Panel A of Table IV.

sensitive to ω_t), causing CDX volatility to increase relative to SPX volatility, with the index volatility ratio increasing to 1.67. For the implied volatility smile, a stochastic ω_t has two effects. The first is to make the return distribution more leptokurtic, which increases the curvature of the smile. The second effect is to generate positive correlation between the index value and variance (both of which depend positively on ω_t), which, other things equal, skews the smile toward higher strikes. Figure 5 (red lines) shows that both implied volatility smiles exhibit more curvature. In addition, for CDX the second effect is sufficiently strong to overturn the leverage effect, resulting in a positively skewed smile.

Third, we add negative correlation between asset returns and volatility ($\omega_t = 0.0135, \sigma_\omega = 0.2, \rho_\omega = -0.70, \lambda_0 = \lambda_\omega = 0$), which adds the third term in (13). This term is positive for CDX (because $\frac{\partial I_t}{\partial A_t} < 0$ and $\frac{\partial I_t}{\partial \omega_t} > 0$) but negative for SPX (because $\frac{\partial I_t}{\partial A_t} > 0$ and $\frac{\partial I_t}{\partial \omega_t} > 0$), so it further increases CDX volatility relative to SPX volatility, with the index volatility ratio increasing to 1.94. For the implied volatility smile, a negative ρ_ω makes the asset return distribution negatively skewed, decreasing SPX return skewness and increasing CDX return skewness (because of opposite signs of $\frac{\partial I_t}{\partial A_t}$), and in turn amplifying the skewed smiles as shown in Figure 5 (yellow lines).

Fourth, we consider the full model with jumps (where the systematic parameters are as in Panel A in Table IV). This shifts systematic risk from diffusive risk toward jump risk. The fourth term in (13) is greater for CDX than SPX, causing the index volatility ratio to increase further to 2.17. For the implied volatility smile, asset value jumps with a negative mean jump size make the asset return distribution both more leptokurtic and negatively skewed, and Figure 5 (purple lines) shows that jumps attenuate the already skewed smiles.

The upshot is that both stochastic volatility and jumps have a significant effect on the relative valuation of CDX and SPX options in terms of both the level and shape of the index implied volatility smiles.

VI. Robustness and Additional Empirical Results

We conduct several robustness checks regarding the LHP approximation, the similarities in the compositions of the CDX and SPX indexes, and the overlap in the asset value states spanned by CDX and SPX options. We also corroborate our model-dependent results on the relative valuation of CDX and SPX options by investigating the investment performance of trading strategies that sell volatility in the two option markets.

A. The LHP Approximation

The LHP approximation of Vasicek (1987) requires that all firms within the index are ex ante identical, so that conditioning on the common systematic state variables, one can apply the law of large numbers. In reality, firms in the CDX and SPX exhibit significant heterogeneity (see below). In Section X of the Internet Appendix, we solve an extension of the model that allows for heterogeneity in leverage across firms. Specifically, we allow for two different groups of firms that are each homogeneous, and we derive analytical solutions to index option prices by using the LHP approximation within each group. We show that, relative to the benchmark model, matching the mean, dispersion, and skewness of the leverage distribution of index constituents leads to lower CDX option prices relative to SPX option prices, hence exacerbating the valuation differential.

Second, the LHP approximation assumes that there are an infinite number of index constituents. In Section XI of the Internet Appendix, we use simulations to price index options for a finite number of index constituents and quantify the bias in the analytical option pricing formulas. We show that the (downward) bias is small, but greater for CDX options than for SPX options because the CDX index has fewer constituents. Therefore, accounting for the actual number of index constituents would raise CDX option prices relative to SPX option prices. However, the effect is small relative to the magnitude of the valuation differential.

B. Comparison of Index Compositions

Our analysis does not require the two indexes to be identical in terms of names, but rather in terms of risk characteristics. To compare the indexes, we focus on four risk characteristics of the underlying constituents that are central to the structural model: rating (as a proxy for the physical-measure default probability), leverage, and total and systematic asset return volatility.[35]

Figure 6 compares the indexes in terms of leverage and ratings. Panels A and B show the distribution of firm-quarter leverage observations for the CDX and SPX constituents, respectively.[36] Clearly, the distribution for SPX constituents has higher dispersion with relatively more low-leverage (even unlevered) and high-leverage firms. However, on average, leverage is similar across the two indexes, with a mean (median) of 0.277 (0.244) for CDX versus 0.238 (0.200) for SPX.

Panels C and D show the distribution of firm-quarter rating observations for the two sets of index constituents.[37] Again, the distribution for SPX constituents has higher dispersion, but for both indexes the mean and median rating is BBB+.[38]

Figure 7 compares the indexes in terms of asset return volatility. Panels A and B show the distribution of firm-quarter observations of total asset return volatility for the CDX and SPX index constituents, respectively. While the distribution for SPX constituents displays slightly higher dispersion (standard deviation of 0.068 for CDX vs. 0.080 for SPX), the average asset volatility is similar, with a mean (median) of 0.167 (0.154) for CDX versus 0.173 (0.158) for SPX.

Since the nondiversifiable component of volatility is the crucial driver of index option value, we plot the distribution of firm-quarter observations of systematic asset return volatility in Panels C and D. These distributions are strikingly similar, with a mean (median) [standard deviation] of 0.092 (0.085) [0.045] for CDX versus 0.098 (0.089) [0.052] for SPX.

Given these results, it seems unlikely that differences in the risk characteristics that drive valuation in our structural model (such as leverage, total volatility, and systematic volatility) can explain our findings. In particular, a potential explanation for the observed price discrepancy between CDX and

[35] Section XII of the Internet Appendix details the computation of asset return volatility. In a nutshell, asset returns are leverage-weighted averages of stock and synthetic bond returns, where stock returns are from the Center for Research in Securities Prices and synthetic bond returns are computed using single-name CDS data from Markit. The systematic component of asset return volatility is obtained from a one-factor model.

[36] In the figure, we focus on total leverage. In the Internet Appendix, we split total leverage into short-term and long-term leverage and find similar results (see Figure IA12). The fraction of CDX (SPX) constituents for which we are able to compute leverage varies between 0.832 and 0.888 (0.892 and 0.984).

[37] Note that ratings data in Compustat are available only up to the third quarter of 2017. During this period, the fraction of CDX (SPX) constituents with ratings information varies between 0.888 and 0.912 (0.864 and 0.892).

[38] When the CDX index is refreshed every six months, it consists only of investment-grade firms (i.e., those rated BBB- and above). The few BB-rated firm-quarter observations in the figure come from firms that were downgraded after index launch.

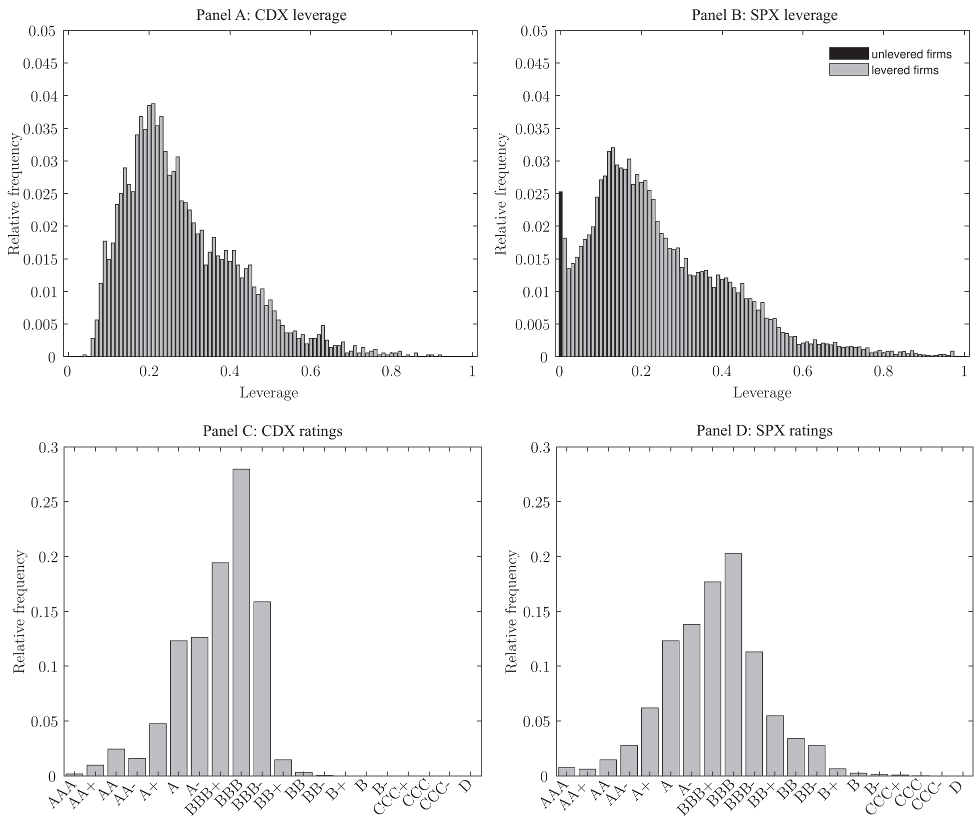

Figure 6. Distributions of leverage and ratings across index constituents. Panels A and B show the distribution of firm-quarter leverage observations for CDX and SPX constituents, respectively, between the first quarter of 2012 and the first quarter of 2020. Leverage is defined as book value of debt over the sum of book value of debt and market value of equity. Panels C and D show the distribution of firm-quarter rating observations for CDX and SPX constituents, respectively, between the first quarter of 2012 and the third quarter of 2017.

SPX options could be relatively higher systematic asset return volatility among CDX constituents, but this is clearly not what we observe in the data.

C. Comparison of Asset Values Spanned by Index Options

The relative pricing argument that we rely on is more palatable if the two option markets span similar economic states.[39] Because CDX and SPX options

[39] Intuitively, if the two markets span different states, then the comparison would rely on "extrapolation" into the tails of the distribution, which might be less robust. For example, Collin-Dufresne, Goldstein, and Yang (2012) show that the effective strike of super-senior CDX tranches is much deeper out of the money than the deepest OTM quoted strike for SPX options, so that relative price comparisons are strongly model dependent.

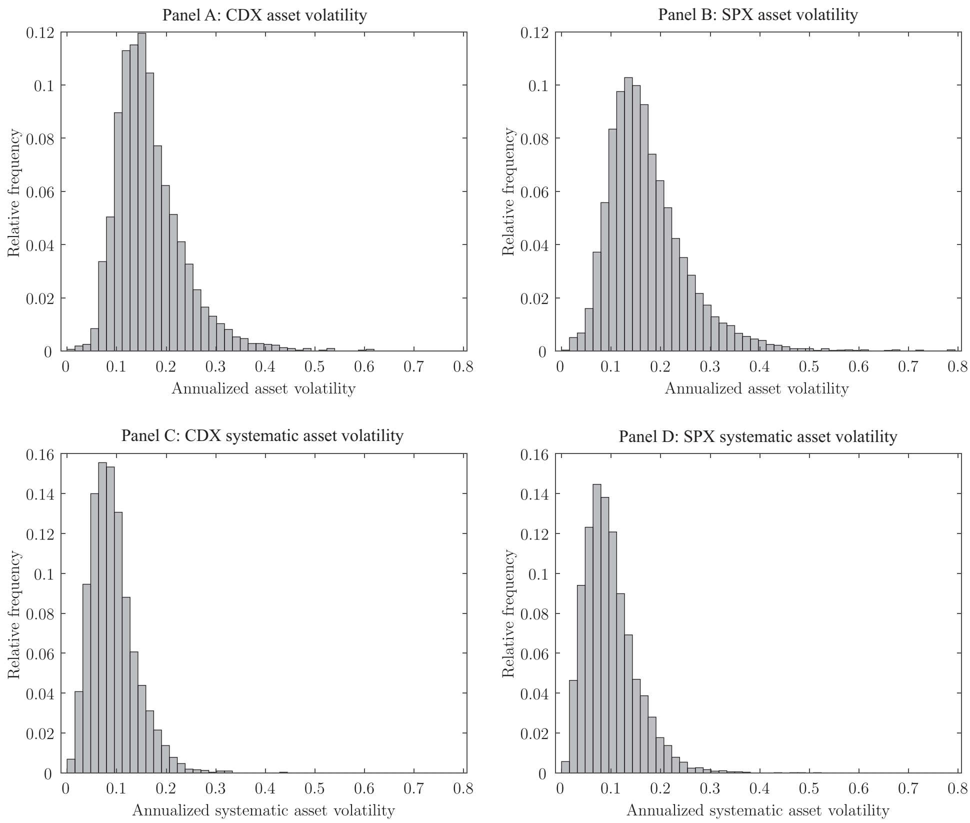

Figure 7. Distributions of asset volatility across index constituents. Panels A and B (C and D) show the distribution of firm-quarter total (systematic) asset return volatility for CDX and SPX constituents, respectively. Asset returns are computed using daily data from January 3, 2012 to December 31, 2019.

are quoted using different models, their strike ranges are not readily comparable. Instead, we translate them into strike ranges in terms of the common asset factor, A_{T_0}. In doing so, we use the model calibrated to SPX options and condition on $\omega = \mathbb{E}_0[\omega_{T_0}]$.

For CDX options, A^{min} is the value of the common factor below which the highest-strike call option expires in the money, and A^{max} is the value above which the lowest-strike put option expires in the money.[40] Similarly, for SPX options, A^{min} is the value of the common factor below which the lowest-strike put option expires in the money, and A^{max} is the value above which the highest-strike call option expires in the money.[41]

[40] Because $U_{T_0}(\log A, \omega)$ is decreasing in A, A^{min} solves $U_{T_0}(\log A^{min}, \omega) = K^{max}$ and A^{max} solves $U_{T_0}(\log A^{max}, \omega) = K^{min}$.

[41] Because $S_{T_0}(\log A, \omega)$ is increasing in A, A^{min} solves $S_{T_0}(\log A^{min}, \omega) = K^{min}$ and A^{max} solves $S_{T_0}(\log A^{max}, \omega) = K^{max}$.

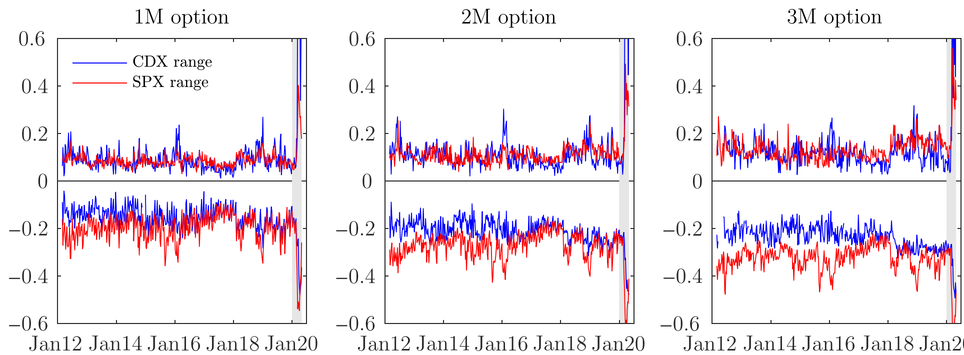

Figure 8. Range of asset values spanned by options. The figure shows $\frac{A^{min}-A^{fwd}}{A^{fwd}}$ and $\frac{A^{max}-A^{fwd}}{A^{fwd}}$ for CDX and SPX options. A^{fwd} is the forward value of the common factor. For CDX options, A^{min} solves $U_{T_0}(\log A^{min}, \omega) = K^{max}$ and A^{max} solves $U_{T_0}(\log A^{max}, \omega) = K^{min}$. For SPX options, A^{min} solves $S_{T_0}(\log A^{min}, \omega) = K^{min}$ and A^{max} solves $S_{T_0}(\log A^{max}, \omega) = K^{max}$. We use the model calibrated to SPX options and always condition on $\omega = \mathbb{E}_0[\omega_{T_0}]$. The sample period is February 29, 2012 to April 29, 2020 (427 weekly observations). The shaded area marks the COVID-19 period starting on January 1, 2020.

Figure 8 plots the time series of the strike range of CDX and SPX options in terms of the common asset factor. Specifically, on each observation date and for each option maturity, we express A^{min} and A^{max} relative to the forward asset value, A^{fwd}; that is, as $\frac{A^{min}-A^{fwd}}{A^{fwd}}$ and $\frac{A^{max}-A^{fwd}}{A^{fwd}}$. Clearly, CDX and SPX options span roughly the same asset values. If anything, the range is greater for SPX options. For instance, for the two-month option maturity, the average strike range is −21.0% to 12.0% for CDX options and −27.4% to 11.4% for SPX options.

D. Trading CDX versus SPX Options

Our model suggests that market prices of CDX options are too expensive relative to SPX options. To corroborate this result, we compare the profitability of selling volatility in the two markets. We consider a strategy of selling ATM straddles within each maturity category on a daily basis and with a holding period of one day (a short holding period ensures that the delta remains close to zero). In addition to holding the option premium in a margin account, we assume that an initial amount of capital is required when selling options. We further assume that the required capital is proportional to the option premium and adjust the proportionality factor to achieve a 10% unconditional annualized volatility of realized excess returns within each option maturity category.[42]

[42] A similar approach is taken in Duarte, Longstaff, and Yu (2007) in their analysis of fixed-income arbitrage strategies. The choice of 10% is inconsequential for our conclusions. Section XIII of the Internet Appendix provides more details on the trading strategy. It also shows that the

Table VI

Summary Statistics of Trading Strategies

In each market and for each option maturity category, the strategy sells closest-to-ATM straddles each trading day with a holding period of one day. We assume that the strategy requires an initial amount of capital proportional to the option premium, and we adjust the proportionality factor to achieve a 10% unconditional annualized volatility of realized excess returns for each option maturity. "EW" denotes an equally weighted portfolio of the three option maturities. "CDX versus SPX options" denotes a short-long strategy that allocates 50% of funds to selling CDX straddles and 50% to buying SPX straddles. Means, standard deviations, and Sharpe ratios ("SR") are annualized. t-Statistics are corrected for heteroskedasticity and serial correlation up to four lags using the approach of Newey and West (1987). The full sample consists of 1,881 daily returns between February 28, 2012 and April 30, 2020. The ex-COVID-19 sample consists of 1,801 daily returns between February 28, 2012 and December 31, 2019.

	CDX Options				SPX Options				CDX versus SPX Options			
	M1	M2	M3	EW	M1	M2	M3	EW	M1	M2	M3	EW
Panel A: Full Sample												
Mean	0.122	0.154	0.189	0.155	0.052	0.073	0.069	0.064	0.035	0.041	0.060	0.045
t-Stat	3.125	3.842	4.742	4.208	1.514	2.052	1.919	1.880	1.865	2.153	3.167	2.623
Std.dev.	0.100	0.100	0.100	0.089	0.100	0.100	0.100	0.098	0.057	0.057	0.057	0.052
SR	1.217	1.539	1.888	1.744	0.515	0.726	0.692	0.659	0.613	0.710	1.051	0.877
Skewness	−2.051	−2.378	−1.493	−2.219	−2.497	−2.277	−2.101	−2.285	−0.236	0.069	0.205	0.142
Kurtosis	14.167	19.322	19.149	17.586	17.593	16.775	15.177	16.125	9.008	10.395	12.045	9.772
Panel B: Ex-COVID-19 Sample												
Mean	0.157	0.206	0.238	0.200	0.081	0.119	0.125	0.108	0.038	0.043	0.057	0.046
t-Stat	4.105	5.344	6.276	5.757	2.418	3.481	3.635	3.269	1.932	2.163	2.815	2.539
Std.dev.	0.100	0.100	0.100	0.087	0.100	0.100	0.100	0.098	0.059	0.059	0.059	0.053
SR	1.568	2.055	2.383	2.291	0.811	1.187	1.248	1.106	0.647	0.731	0.963	0.868
Skewness	−1.802	−1.781	−1.122	−1.717	−2.598	−2.285	−1.980	−2.314	−0.327	0.020	0.175	0.072
Kurtosis	12.718	14.466	19.333	14.476	19.176	18.696	15.770	17.950	9.399	10.810	12.372	10.226

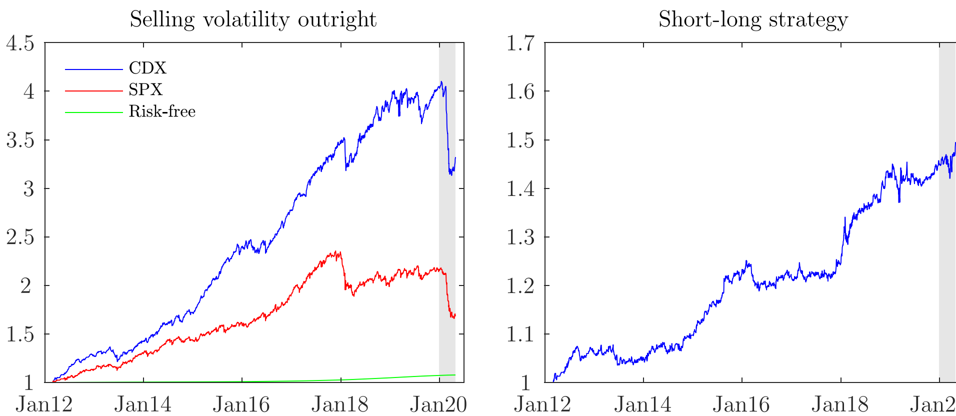

Figure 9. Cumulative performance of trading strategies. The figure shows the evolution of one dollar invested in each of the EW strategies at the beginning of the sample (see Table VI for details on the trading strategies). The left panel shows the performance of selling CDX and SPX straddles outright. The right panel shows the performance of the short-long strategy that allocates 50% of funds to selling CDX straddles and 50% to buying SPX straddles. On those trading days when option returns are not available, we invest at the risk-free rate. The sample period is from February 24, 2012 to April 30, 2020 (2,042 daily observations). The shaded area marks the COVID-19 period starting on January 1, 2020.

Table VI shows summary statistics of returns for each option maturity as well as for an equally weighted (EW) portfolio of the three option maturities.[43] Across all maturities and both including and excluding the COVID-19 crisis, selling CDX volatility generates higher and more statistically significant average excess returns and higher Sharpe ratios than selling SPX volatility. For instance, for the full sample (Panel A), the EW portfolio generates an annualized Sharpe ratio of 1.744 in the CDX market versus 0.659 in the SPX market. Because of the large increase in volatility during the COVID-19 crisis, the strategy in both markets performs better during the ex-COVID-19 sample (Panel B).[44]

We also consider a short-long strategy of selling CDX straddles versus buying SPX straddles.[45] This strategy generates Sharpe ratios that are typically higher than those of selling SPX volatility outright, but lower than selling CDX

results are robust to assuming that the required capital is constant over time (rather than varying with the option premium).

[43] When computing performance, we only consider returns on those days when returns are available for all option maturities and for both markets.

[44] A contemporaneous paper by Ammann and Moerke (2023) constructs synthetic variance swap contracts from CDX options and finds that selling CDX variance swaps generates higher Sharpe ratios than selling SPX variance swaps in a pre-COVID-19 sample. See also Chen, Doshi, and Seo (2023).

[45] We assume that the same amount of capital is required when buying SPX straddles as when selling them, so that we maintain a 10% unconditional annualized volatility of realized excess returns. The short-long strategy then allocates 50% of funds to selling CDX straddles and 50% to buying SPX straddles.

volatility outright. For instance, for the full sample, trading the EW portfolios against each other generates an annualized Sharpe ratio of 0.877. Furthermore, the higher-order moments of the long-short strategy are more attractive, with the return distributions roughly symmetric (instead of highly negatively skewed) and much less leptokurtic. Figure 9 shows the evolution of one dollar invested in each of the EW strategies at the beginning of the sample. Clearly, the short-long strategy avoids the occasional large drawdowns from selling volatility outright.

VII. Conclusion

In recent years, a liquid market for credit index (CDX) options has developed. We study the extent to which these options are priced consistent with S&P 500 (SPX) equity index options. We consider a rich structural credit-risk model in which both idiosyncratic and systematic asset risk have a diffusive component and a jump component, and the common factor exhibits stochastic volatility and a variance-dependent jump intensity. Using the large homogeneous portfolio approximation and new results on multivariate transform analysis for affine processes, we obtain analytical solutions to indexes and index options, which are compound options in our structural modeling framework. Estimating the model, we find that it captures many aspects of the joint dynamics of CDX and SPX options. However, according to the model, market prices of CDX options are too expensive relative to SPX options, suggesting that credit and equity markets are not fully integrated—at least not in the strong sense suggested by classic Merton (1974)-style structural models, where both credit and equity options are priced by the same set of risk factors that drive the asset value process. This result is further corroborated by a model-independent analysis of option trading strategies, which shows that selling CDX volatility yields significantly higher average excess returns and Sharpe ratios than selling SPX volatility.

Our findings suggest at least two lines of future research. First, although our model incorporates salient features of asset value dynamics, it can surely be extended further, for instance, by adding multifactor systematic and idiosyncratic stochastic volatility, or by allowing for a more complex default boundary.[46] Of particular interest would be to incorporate credit-specific risk factors. A natural candidate for such a factor would be systematic variation in bankruptcy costs; in Section XIV of the Internet Appendix we show how to add this feature while keeping analytical expressions for all derivatives prices.[47] Whether these and other model extensions can account for the observed discrepancy between CDX and SPX option prices is an open question.

[46] For example, in a paper subsequent to ours, Doshi et al. (2021) explore whether a first-passage-time structural model with priced asset variance risk can reconcile pricing across CDX and SPX option markets.

[47] Another plausible candidate would be a credit-specific liquidity factor, as suggested by Bao and Pan (2013) and Friewald and Nagler (2019).

Another line of research would be searching for institutional features that can cause market segmentation and a persistent price discrepancy. For instance, Basel III regulation has created significant demand for CDX call options from banks that seek to hedge their credit valuation adjustment (CVA) exposures in order to reduce their regulatory capital.[48] Using regulatory filings on risk-weighted assets for CVA from eight global systemically important U.S. banks, we show in Section XV of the Internet Appendix that the size of this hedging demand could potentially account for a large fraction of the trading activity in CDX options. Thus, demand pressure, along the lines of Gârleanu, Pedersen, and Poteshman (2009), could distort the relative prices of CDX and SPX options.

Initial submission: February 17, 2021; Accepted: October 29, 2022
Editors: Stefan Nagel, Philip Bond, Amit Seru, and Wei Xiong

Appendix: Proofs

A. Dynamics of the State Variables

We can rewrite the individual firm asset value as

$$A_T^i = A_T e^{-\frac{1}{2}\sigma_i{}^2 T + \sigma_i W_T^i} e^{-\lambda_i \nu_i T + \sum_{j=1}^{N_T^i} \gamma_{i,j}}, \tag{A.1}$$

where the common factor $a_t = \log A_t$ has dynamics

$$da_t = \left(r - \delta - \lambda_t \nu - \frac{1}{2}\omega_t \right) dt + \sqrt{\omega_t} dW_t + \gamma dN_t. \tag{A.2}$$

Note that the state vector

$$x_t = [a_t, \omega_t]^\top$$

follows an affine jump-diffusion process.

It is helpful to define $a_T^i = \log A_T^i = a_T + \xi_T^i$ with

$$d\xi_t^i = -\left(\frac{1}{2}\sigma_i{}^2 + \lambda_i \nu_i \right) dt + \sigma_i dW_t^i + \gamma_i dN_t^i, \tag{A.3}$$

so that $A_t^i = e^{a_t + \xi_t^i}$, and $M_t^i = e^{\xi_t^i}$ is a strictly positive martingale. Then the state when considering a specific firm can be defined as

$$x_t^i = \left[a_t, \omega_t, \xi_t^i \right]^\top.$$

[48] In the aftermath of the financial crisis, the Basel III regulation introduced a new capital charge—the CVA risk charge—to cover the risk of deterioration in the creditworthiness of counterparties. Both CDX and CDX options are eligible hedge instruments, but due to a discrepancy between the regulatory and accounting treatment of counterparty risk, many banks prefer to use CDX options (see, e.g., Becker (2014)).

We note that the ξ_t^i are independent of x_t, and the A_T^i have i.i.d. distributions conditional on x_T, which will be helpful when deriving CDX and SPX values.

B. Proof of Theorem 1

The theorem follows directly from applying theorems 5 and 6 of Shephard (1991) to recover the cumulative joint distribution of the n random variables $x_j := \beta_j \cdot X_{T_j} \forall j = 1, \ldots, n$ under the $\mathbb{P}^\alpha$ measure, i.e., $G_\beta^\alpha(y_1, \ldots, y_n) = \mathbb{P}^\alpha(x_1 \leq y_1, \ldots, x_n \leq y_n)$, from its characteristic function defined as

$$\begin{aligned}\varphi(u_1, \ldots, u_n) &= \mathbb{E}^\alpha\left[e^{\mathrm{i}(u_1 x_1 + \cdots + u_n x_n)}\right] \\ &= \Psi^\alpha(\mathrm{i}u_1\beta_1, \ldots, \mathrm{i}u_n\beta_n; \overline{X}_{T_0}, T_0, T_1, \ldots, T_n),\end{aligned}$$

where the moment-generating function can be computed as follows $\forall j \geq 1$:

$$\begin{aligned}\Psi^\alpha(\beta_1, \ldots, \beta_j; \overline{X}_{T_0}, T_0, T_1, \ldots, T_j) &:= \mathbb{E}^\alpha\left[e^{\beta_1 \cdot X_{T_1} + \cdots + \beta_j \cdot X_{T_j}} \,|\, \overline{X}_{T_0}\right] \\ &= \frac{1}{\Psi(\alpha; \overline{X}_{T_0}, T_0, T_j)} \mathbb{E}\left[e^{\beta_1 \cdot X_{T_1} + \cdots + (\beta_j + \alpha) \cdot X_{T_j}} \,|\, \overline{X}_{T_0}\right] \\ &= \frac{\Psi(\beta_1, \ldots, \beta_{j-1}, \beta_j + \alpha; \overline{X}_{T_0}, T_0, T_1, \ldots, T_j)}{\Psi(\alpha; \overline{X}_{T_0}, T_0, T_j)}.\end{aligned}$$

For any set of N-dimensional vectors β_j, $j = 1, \ldots, n$, we have

$$\begin{aligned}\Psi(\beta_1, \ldots, \beta_j; \overline{X}_{T_0}, T_0, T_1, \ldots, T_j) &:= \mathbb{E}\left[e^{\beta_1 \cdot X_{T_1} + \cdots + \beta_j \cdot X_{T_j}} \,|\, \overline{X}_{T_0}\right] \\ &= \mathbb{E}\left[e^{\beta_1 \cdot X_{T_1} + \cdots + \beta_{j-1} \cdot X_{T_{j-1}}} \mathbb{E}\left[e^{\beta_j \cdot X_{T_j}} \,|\, X_{T_{j-1}}\right] \,|\, \overline{X}_{T_0}\right] \\ &= \mathbb{E}\left[e^{\beta_1 \cdot X_{T_1} + \cdots + \beta_{j-1} \cdot X_{T_{j-1}}} \Psi(\beta_j; X_{T_{j-1}}, T_{j-1}, T_j) \,|\, \overline{X}_{T_0}\right] \\ &= \mathbb{E}\left[e^{\beta_1 \cdot X_{T_1} + \cdots + \beta_{j-1} \cdot X_{T_{j-1}}} e^{b_{\beta_j}(T_{j-1}, T_j) + c_{\beta_j}(T_{j-1}, T_j) \cdot X_{T_{j-1}}} \,|\, \overline{X}_{T_0}\right] \\ &= \Psi(\beta_1, \ldots, \beta_{j-2}, \beta_{j-1} + c_{\beta_j}(T_{j-1}, T_j); \overline{X}_{T_0}, T_0, T_1, \ldots, T_{j-1}) \\ &\quad \times e^{b_{\beta_j}(T_{j-1}, T_j)}.\end{aligned}$$

We thus obtain an explicit recursive solution for the relevant multivariate characteristic function in terms of the two deterministic functions $b_\beta(t, T)$ and $c_\beta(t, T)$ in (12).

C. Proof of Theorem 2

To prove the first result, we have

$$\Psi(\beta; x_t^i, t, T) := \mathbb{E}\left[e^{\beta \cdot x_T^i} \,|\, x_t^i\right]$$

$$
\begin{aligned}
&= \mathbb{E}\left[e^{\beta_1 a_T + \beta_2 \omega_T + \beta_3 \xi_T^i} \mid x_t^i\right] \\
&= \mathbb{E}\left[e^{\beta_3 \xi_T^i} \mid \xi_t^i\right] \mathbb{E}\left[e^{\beta_1 a_T + \beta_2 \omega_T} \mid x_t\right] \\
&= e^{\beta_3 \xi_t^i + \zeta(\beta_3)(T-t) + \beta_1 a_t + B(T-t;\beta_1,\beta_2) + C(T-t;\beta_1,\beta_2)\omega_t},
\end{aligned}
$$

where we use the fact that ξ_t^i is independent of a_t and ω_t, and the final expression obtains from Lemmas A.1 and A.2.

To prove the second result, we proceed similarly:

$$
\begin{aligned}
\Psi(\beta; x_t, t, T) &:= \mathbb{E}\left[e^{\beta \cdot x_T^i} \mid x_t\right] \\
&= \mathbb{E}\left[e^{\beta_1 a_T + \beta_2 \omega_T + \beta_3 \xi_T^i} \mid x_t\right] \\
&= \mathbb{E}\left[e^{\beta_3 \xi_T^i}\right] \mathbb{E}\left[e^{\beta_1 a_T + \beta_2 \omega_T} \mid x_t\right] \\
&= e^{\zeta(\beta_3) T + \beta_1 a_t + B(T-t;\beta_1,\beta_2) + C(T-t;\beta_1,\beta_2)\omega_t}.
\end{aligned}
$$

LEMMA A.1:

$$
\mathbb{E}\left[e^{\beta_3 \xi_T^i} \mid \xi_t^i\right] = e^{\beta_3 \xi_t^i + \zeta(\beta_3)(T-t)},
$$

where

$$
\zeta(\beta_3) = -\frac{1}{2}{\sigma_i}^2 \beta_3 (1-\beta_3) - \lambda_i(\beta_3 \nu_i - \nu^i(\beta_3)) \tag{A.4}
$$

and (for some scalar β)

$$
\nu^i(\beta) = \mathbb{E}\left[e^{\gamma_i \beta} - 1\right] = e^{m_i \beta + \frac{1}{2} v_i \beta^2} - 1.
$$

PROOF: Follows from the definition of ξ_t^i in equation (A.3). □

LEMMA A.2:

$$
\mathbb{E}\left[e^{\beta_1 a_T + \beta_2 \omega_T} \mid x_t\right] = e^{\beta_1 a_t + B(T-t;\beta_1,\beta_2) + C(T-t;\beta_1,\beta_2)\omega_t},
$$

where $B(T-t;\beta_1,\beta_2)$ and $C(T-t;\beta_1,\beta_2)$ are deterministic functions given below.

PROOF: Using the law of iterated expectation, we seek a candidate solution $M_t = e^{\beta_1 a_t + B(T-t) + C(T-t)\omega_t}$ that is a martingale. That is, $\mathbb{E}_t[\frac{dM_t}{M_{t^-}}] = 0$ or equivalently

$$
\begin{aligned}
0 = &- \dot{B} - \dot{C}\omega_t + \beta_1\left(r - \delta - \frac{1}{2}\omega_t\right) - \beta_1(\lambda_0 + \lambda_\omega \omega_t)\nu + C\kappa(\bar{\omega} - \omega_t) \\
&+ \frac{1}{2}\beta_1^2 \omega_t + \frac{1}{2}C^2 \sigma_\omega^2 \omega_t + \beta_1 C \rho_\omega \sigma_\omega \omega_t + (\lambda_0 + \lambda_\omega \omega_t)\nu(\beta_1),
\end{aligned}
$$

where (for some scalar β)

$$\nu(\beta) = \mathbb{E}\left[e^{\gamma\beta} - 1\right] = e^{m\beta + \frac{1}{2}\upsilon\beta^2} - 1.$$

This implies the following system of ordinary differential equations:

$$\dot{B} = \beta_1(r - \delta) + \lambda_0(\nu(\beta_1) - \beta_1\nu) + \kappa\bar{\omega}C$$
$$\dot{C} = P - QC + \frac{1}{2}\sigma_\omega^2 C^2,$$

where

$$P = \frac{1}{2}\beta_1(\beta_1 - 1) + \lambda_\omega(\nu(\beta_1) - \beta_1\nu)$$
$$Q = \kappa - \beta_1\rho_\omega\sigma_\omega,$$

which must be solved subject to the boundary conditions $B(0) = 0$ and $C(0) = \beta_2$. The solution is given by

$$B(\tau) = \beta_1(r - \delta)\tau + \lambda_0(\nu(\beta_1) - \beta_1\nu)\tau + \frac{\kappa\bar{\omega}}{\sigma_\omega^2}\left((Q - d)\tau - 2\log\left(\frac{1 - ce^{-d\tau}}{1 - c}\right)\right), \tag{A.5}$$

$$C(\tau) = \frac{(Q - d) - (Q + d)ce^{-d\tau}}{\sigma_\omega^2(1 - ce^{-d\tau})}, \tag{A.6}$$

where

$$d = \sqrt{Q^2 - 2P\sigma_\omega^2},$$
$$c = \frac{Q - d - \beta_2\sigma_\omega^2}{Q + d - \beta_2\sigma_\omega^2}.$$

□

REFERENCES

Ammann, Manuel, and Mathis Moerke, 2023, Credit variance risk premiums, *European Financial Management* 29, 1304–1335.

Andrade, Gregor, and Steven N. Kaplan, 1998, How costly is financial (not economic) distress? Evidence from highly leveraged transactions that became distressed, *Journal of Finance* 53, 1443–1494.

Bai, Jennie, Turan G. Bali, and Quan Wen, 2019, Common risk factors in the cross-section of corporate bond returns, *Journal of Financial Economics* 131, 619–642.

Bai, Jennie, Robert S. Goldstein, and Fan Yang, 2019, The leverage effect and the basket-index put spread, *Journal of Financial Economics* 131, 186–205.

Bao, Jack, and Jun Pan, 2013, Bond illiquidity and excess volatility, *Review of Financial Studies* 26, 3068–3103.

Becker, Lucas, 2014, CVA hedge losses prompt focus on swaptions and guarantees, *Risk Magazine*.

Black, Fischer, and John C. Cox, 1976, Valuing corporate securities: Some effects of bond indenture provisions, *Journal of Finance* 31, 351–367.

Broadie, Mark, Mikhail Chernov, and Michael Johannes, 2007, Model specification and risk premia: Evidence from futures options, *Journal of Finance* 62, 1453–1490.

Carr, Peter, and Liuren Wu, 2010, Stock options and credit default swaps: A joint framework for valuation and estimation, *Journal of Financial Econometrics* 8, 409–449.

Chen, Long, Pierre Collin-Dufresne, and Robert S. Goldstein, 2009, On the relation between the credit spread puzzle and the equity premium puzzle, *Review of Financial Studies* 22, 3367–3409.

Chen, Steven Shu-Hsi, Hitesh Doshi, and Sang Byung Seo, 2023, Synthetic options and implied volatility for the corporate bond market, *Journal of Financial and Quantitative Analysis* 58, 1295–1325.

Chen, Zhiwu, and Peter J. Knez, 1995, Measurement of market integration and arbitrage, *Review of Financial Studies* 8, 287–325.

Choi, Jaewon, and Yongjun Kim, 2018, Anomalies and market (dis)integration, *Journal of Monetary Economics* 100, 16–34.

Chordia, Tarun, Amit Goyal, Yoshio Nozawa, Avanidhar Subrahmanyam, and Qing Tong, 2017, Are capital market anomalies common to equity and corporate bond markets? An empirical investigation, *Journal of Financial and Quantitative Analysis* 52, 1301–1342.

Collin-Dufresne, Pierre, Robert S. Goldstein, and J. Spencer Martin, 2001, The determinants of credit spread changes, *Journal of Finance* 56, 2177–2207.

Collin-Dufresne, Pierre, Robert S. Goldstein, and Fan Yang, 2012, On the relative pricing of long-maturity index options and collateralized debt obligations, *Journal of Finance* 67, 1983–2014.

Collin-Dufresne, Pierre, Benjamin Junge, and Anders B. Trolle, 2020, Market structure and transaction costs of index CDSs, *Journal of Finance* 75, 2719–2763.

Coval, Joshua, Jakub Jurek, and Erik Stafford, 2009, Economic catastrophe bonds, *American Economic Review* 99, 628–666.

Cremers, Martijn, Joost Driessen, and Pascal Maenhout, 2008, Explaining the level of credit spreads: Option-implied jump risk premia in a firm value model, *Review of Financial Studies* 21, 2209–2242.

Culp, Christopher L., Yoshio Nozawa, and Pietro Veronesi, 2018, Option-based credit spreads, *American Economic Review* 108, 454–488.

Davydenko, Sergei A., Ilya A. Strebulaev, and Xiaofei Zhao, 2012, A market-based study of the cost of default, *Review of Financial Studies* 25, 2959–2999.

Doshi, Hitesh, Jan Ericsson, Mathieu Fournier, and Sang Byung Seo, 2021, Asset variance risk and compound option prices, Working paper, McGill University.

Du, Du, Redouane Elkamhi, and Jan Ericsson, 2019, Time-varying asset volatility and the credit spread puzzle, *Journal of Finance* 74, 1841–1885.

Duarte, Jefferson, Francis A. Longstaff, and Fan Yu, 2007, Risk and return in fixed-income arbitrage: Nickels in front of a steamroller? *Review of Financial Studies* 20, 769–811.

Duffie, Darrell, Damir Filipović, and Walter Schachermayer, 2003, Affine processes and applications in finance, *Annals of Applied Probability* 13, 984–1053.

Duffie, Darrell, Jun Pan, and Kenneth J. Singleton, 2000, Transform analysis and asset pricing for affine jump-diffusions, *Econometrica* 68, 1343–1376.

Fama, Eugene F., 1970, Efficient capital markets: A review of theory and empirical work, *Journal of Finance* 25, 383–417.

Foresi, Silverio, and Liuren Wu, 2005, Crash-o-phobia: A domestic fear or a worldwide concern? *Journal of Derivatives* 13, 8–21.

Friewald, Nils, and Florian Nagler, 2019, Over-the-counter market frictions and yield spread changes, *Journal of Finance* 74, 3217–3257.

Gârleanu, Nicolae, Lasse H. Pedersen, and Allen M. Poteshman, 2009, Demand-based option pricing, *Review of Financial Studies* 22, 4259–4299.

Geske, Robert, 1977, The valuation of corporate liabilities as compound options, *Journal of Financial and Quantitative Analysis* 12, 541–552.

Gil-Pelaez, J., 1951, Note on the inversion theorem, *Biometrika* 38, 481–482.

He, Zhiguo, Paymon Khorrami, and Zhaogang Song, 2022, Commonality in credit spread changes: Dealer inventory and intermediary distress, *Review of Financial Studies* 35, 4630–4673.

Huang, Jing-Zhi, and Ming Huang, 2012, How much of the corporate-treasury yield spread is due to credit risk? *Review of Asset Pricing Studies* 2, 153–202.

Jones, Philip E., Scott P. Mason, and Eric Rosenfeld, 1984, Contingent claims analysis of corporate capital structures: An empirical investigation, *Journal of Finance* 39, 611–625.

Kapadia, Nikunj, and Xiaoling Pu, 2012, Limited arbitrage between equity and credit markets, *Journal of Financial Economics* 105, 542–564.

Leland, Hayne E., 1994, Optimal capital structure, endogenous bankruptcy, and the term structure of credit spreads, *Journal of Finance* 49, 1213–1252.

Merton, Robert C., 1974, On the pricing of corporate debt: The risk structure of interest rates, *Journal of Finance* 29, 449–470.

Newey, Whitney K., and Kenneth D. West, 1987, A simple, positive semi-definite, heteroskedasticity and autocorrelation consistent covariance matrix, *Econometrica* 55, 703–708.

Sandulescu, Mirela, 2020, How integrated are corporate bond and stock markets? Working paper, University of Michigan.

Schaefer, Stephen M., and Ilya A. Strebulaev, 2008, Structural models of credit risk are useful: Evidence from hedge ratios on corporate bonds, *Journal of Financial Economics* 90, 1–19.

Seo, Sang Byung, and Jessica Wachter, 2018, Do rare events explain CDX tranche spreads? *Journal of Finance* 73, 2343–2383.

Shephard, Neil, 1991, From characteristic function to distribution function: A simple framework for the theory, *Econometric Theory* 7, 519–529.

Vasicek, Oldrich, 1987, Probability of loss on a loan portfolio, KMV Corporation.

Supporting Information

Additional Supporting Information may be found in the online version of this article at the publisher's website:

Appendix S1: Internet Appendix.
Replication Code.